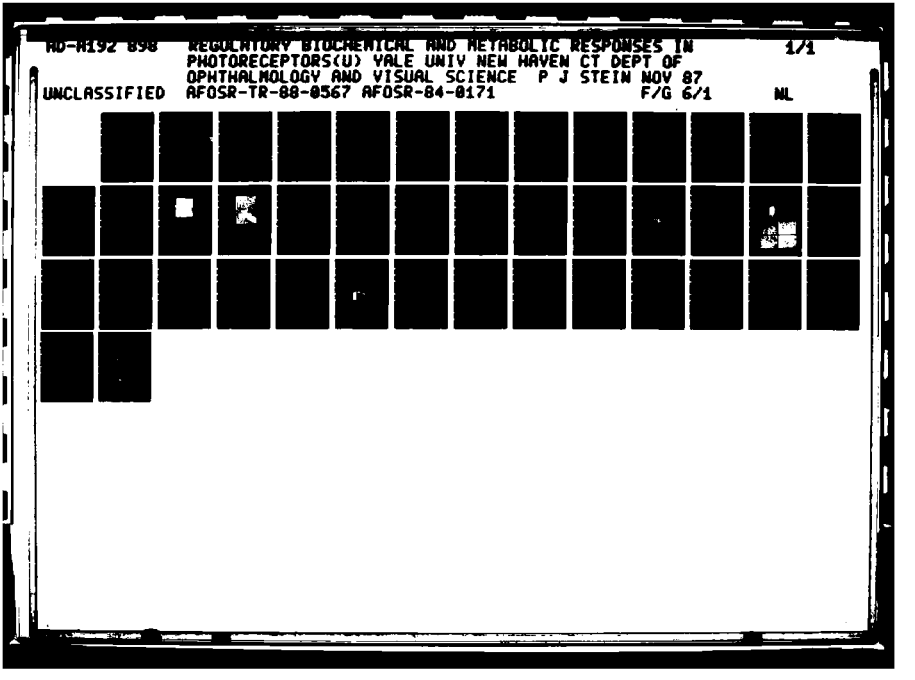
AD-A192 898 REGULATORY BIOCHEMICAL AND METABOLIC RESPONSES IN PHOTORECEPTORS(U) YALE UNIV NEW HAVEN CT DEPT OF OPHTHALMOLOGY AND VISUAL SCIENCE P J STEIN NOV 87
UNCLASSIFIED AFOSR-TR-88-0567 AFOSR-84-0171 F/G 6/1 NL

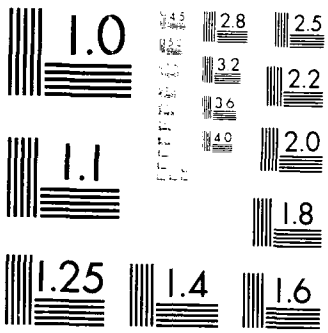
1.0
1.1
1.25
1.4
1.6
1.8
2.0
2.2
2.5
2.8
3.2
3.6
4.0

UNCLASSIFIED DTIC FILE COPY

SECURITY CLASSIFICATION OF THIS PAGE

REPORT DOCUMENTATION PAGE

AD-A192 898

1b. RESTRICTIVE MARKINGS

3. DISTRIBUTION/AVAILABILITY OF REPORT
Approved for public release; distribution unlimited.

2b. DECLASSIFICATION/DOWNGRADING SCHEDULE

4. PERFORMING ORGANIZATION REPORT NUMBER(S)

5. MONITORING ORGANIZATION REPORT NUMBER(S)
AFOSR-TR- 88-0567

6a. NAME OF PERFORMING ORGANIZATION
Yale University Sch. of Med.

6b. OFFICE SYMBOL (If applicable)

7a. NAME OF MONITORING ORGANIZATION
Air Force Office of Scientific Research

6c. ADDRESS (City, State and ZIP Code)
Yale University School of Medicine
333 Cedar Street
New Haven, CT 06510

7b. ADDRESS (City, State and ZIP Code)
AFOSR/NL
Building 410
Bolling Air Force Base DC 20332-6418

8a. NAME OF FUNDING/SPONSORING ORGANIZATION
AFOSR

8b. OFFICE SYMBOL (If applicable)
NL

9. PROCUREMENT INSTRUMENT IDENTIFICATION NUMBER
AFOSR-84-0171

8c. ADDRESS (City, State and ZIP Code)
Bldg. 410
Bolling AFB, DC 20332-6448

10. SOURCE OF FUNDING NOS.

PROGRAM ELEMENT NO.	PROJECT NO.	TASK NO.	WORK UNIT NO.
61102F	2312	A2	

11. TITLE (Include Security Classification) Regulatory Biochemical and Metabolic Responses in Photoreceptors

12. PERSONAL AUTHOR(S)
Peter J. Stein

13a. TYPE OF REPORT	13b. TIME COVERED	14. DATE OF REPORT (Yr., Mo., Day)	15. PAGE COUNT
Final	FROM 7/1/84 TO 9/30/87	November 30, 1987	39

16. SUPPLEMENTARY NOTATION

17. COSATI CODES			18. SUBJECT TERMS (Continue on reverse if necessary and identify by block number)
FIELD	GROUP	SUB GR	Photoreceptors, Rods, G-protein, Nucleotides, Light Scattering, Channels

19. ABSTRACT (Continue on reverse if necessary and identify by block number)

Studies of near infrared light scattering changes in disk membrane suspensions revealed three novel phenomena. The light induced scattering changes observed in the presence of GTP and cGMP were produced by aggregation/disaggregation of the membrane vesicles. This aggregation/disaggregation process was correlated with activation of phosphodiesterase and a change in its apparent solubility. That is, PDE became more tightly bound to the membrane when it was activated. We have begun preliminary studies of near infrared scattering signals in the isolated retina. In this preliminary work, we have observed that IBMX, an inhibitor of phosphodiesterase activity, profoundly affects the infrared light scattering signal in the isolated retina. It seems likely that the in vitro and in vivo signals may share a common origin.

In a separate series of experiments, we have purified opsin, the apoprotein of the visual pigment protein, and reconstituted it into phospholipid vesicles. We used patch clamp recording to demonstrate that the purified, reconstituted protein exhibits cGMP-activated

20. DISTRIBUTION/AVAILABILITY OF ABSTRACT
UNCLASSIFIED/UNLIMITED ☐ SAME AS RPT. ☐ DTIC USERS ☐

21. ABSTRACT SECURITY CLASSIFICATION

22a. NAME OF RESPONSIBLE INDIVIDUAL	22b. TELEPHONE NUMBER (Include Area Code)	22c. OFFICE SYMBOL
Dr. William O. Berry	202/767-5021	NL

DD FORM 1473, 83 APR EDITION OF 1 JAN 73 IS OBSOLETE. UNCLASSIFIED
SECURITY CLASSIFICATION OF THIS PAGE

19

27 APR 1988

DTIC ELECTE MAY 19 1988 S E D

19. Abstract (continued)

single channel activity. These results suggest that opsin, in addition to performing its function as the receptor molecule, may be the light-sensitive pore in the plasma membrane of the rod outer segment.

Final Report: Regulatory Biochemical and Metabolic Responses in Photoreceptors

AFOSR Grant #84-0171
7/1/84-9/30/87
P.I. Peter J. Stein
Department of Ophthalmology and Visual Science
Yale University School of Medicine
New Haven, CT 06510

1. Summary:

The experiments performed during the period of this research grant resulted in a number of important new insights into the molecular events which occur as a result of photoisomerization of rhodopsin. These events were studied with infrared light scattering, by study of protein binding and release from disk membranes, by phase contrast microscopy, and enzymologically. In parallel experiments, we measured light scattering changes in the isolated, superfused retina. The signal generated in the retina was studied with different pharamacological treatments to relate it to the in vitro signal observed in disk membrane suspensions. The results of these experiments indicated that there was a GTP- and cGMP-dependent infrared light scattering signal in rod disk membrane suspensions. This signal was elicited by very low bleaching flashes and results from enhanced vesicle-vesicle aggregation. The aggregation process was correlated with activation of cGMP phosphodiesterase (PDE) by G-protein and by enhanced binding of PDE to the disk membrane. In the isolated retina, the infrared light scattering signal which we studied was greatly altered by inhibitors of cGMP hydrolysis. Therefore, it seems likely to be related to the GTP- and cGMP-dependent signal obseved in vitro.

Finally, we have purified opsin, reconstituted it into freeze thaw liposomes and used patch clamp recording to demonstrate that opsin exhibits cGMP-dependent single channel activity. Two elementary conductances, of 17 and 32 pS, were observed in the presence of 10-200 uM cGMP. These results suggest that opsin, in addition to performing as the receptor molecule, may be the light-sensitive pore as well.

2. Research Objectives:

A. To construct a microspectrophotometer capable of recording optical changes in single photoreceptor cells.

B. To record and characterize light scattering signals in the retina under different light intensity and pharmacological conditions.

C. To characterize light scattering changes in rod disk membranes and in reconstituted membrane/enzyme systems.

3. Status of Research:

In our initial attempts to study rhodopsin/G-protein interactions using near infrared light scattering, we were unable to reproduce the siganls reported by Kuhn et al., 1983 (See figure 1, trace a). We were able to reproduce their results by utilizing purified G-protein recombined with washed disk membranes. Figure 2A, traces a and b show the Binding and Dissociation signals, respectively. The remaining traces in Figure 2, c-e, show that there were additional components to the light scattering signal which depended upon the presence of cGMP and PDE, in addition to bleached rhodopsin, G-protein, and GTP.

The cGMP- and PDE-dependent light scattering signal is complex, as is illustrated in Figure 2A, trace e. Figure 2B shows the effect of adding increasing amounts of PDE to a reconstituted system containing G-protein, GTP, and rhodopsin. The D-phase of the signal became larger

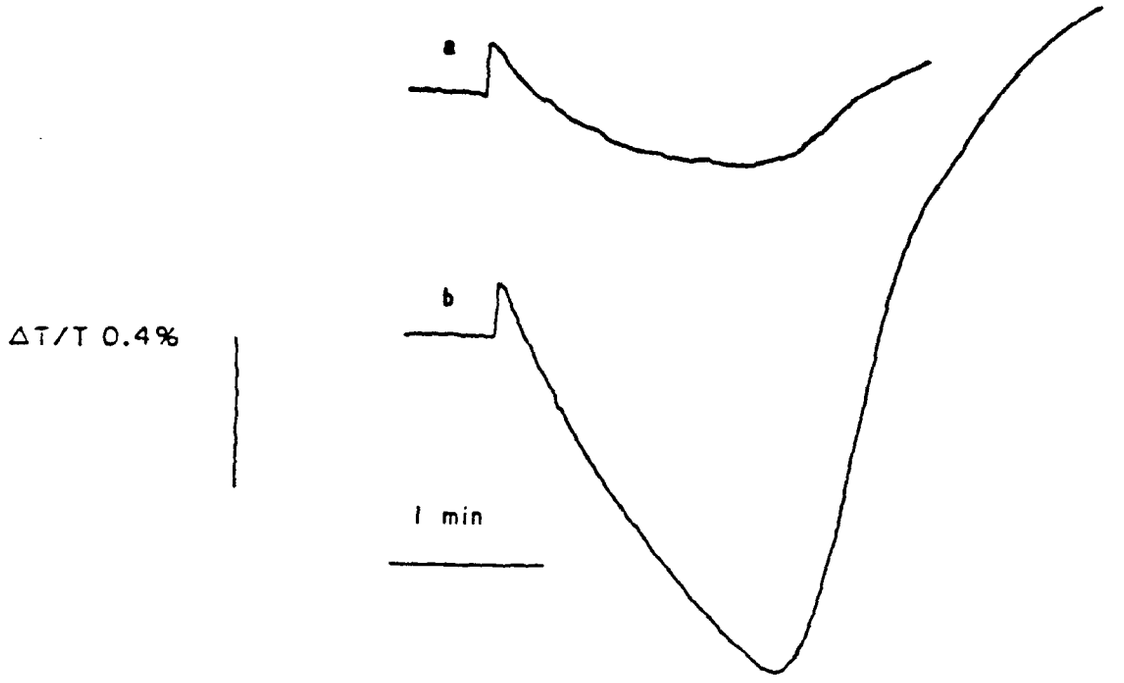

FIGURE 1: Near-infrared light-scattering changes of a suspension of disrupted disk membranes. Stacked disks were disrupted by passing them through a 25-gauge syringe needle as described under Materials and Methods. [Rhodopsin] = 2 μM. The flash (indicated by the arrow) bleached 0.2% rhodopsin. Trace a, [GTP] = 2 μM, no cGMP; trace b, [GTP] = 2 μM, [cGMP] = 1 mM.

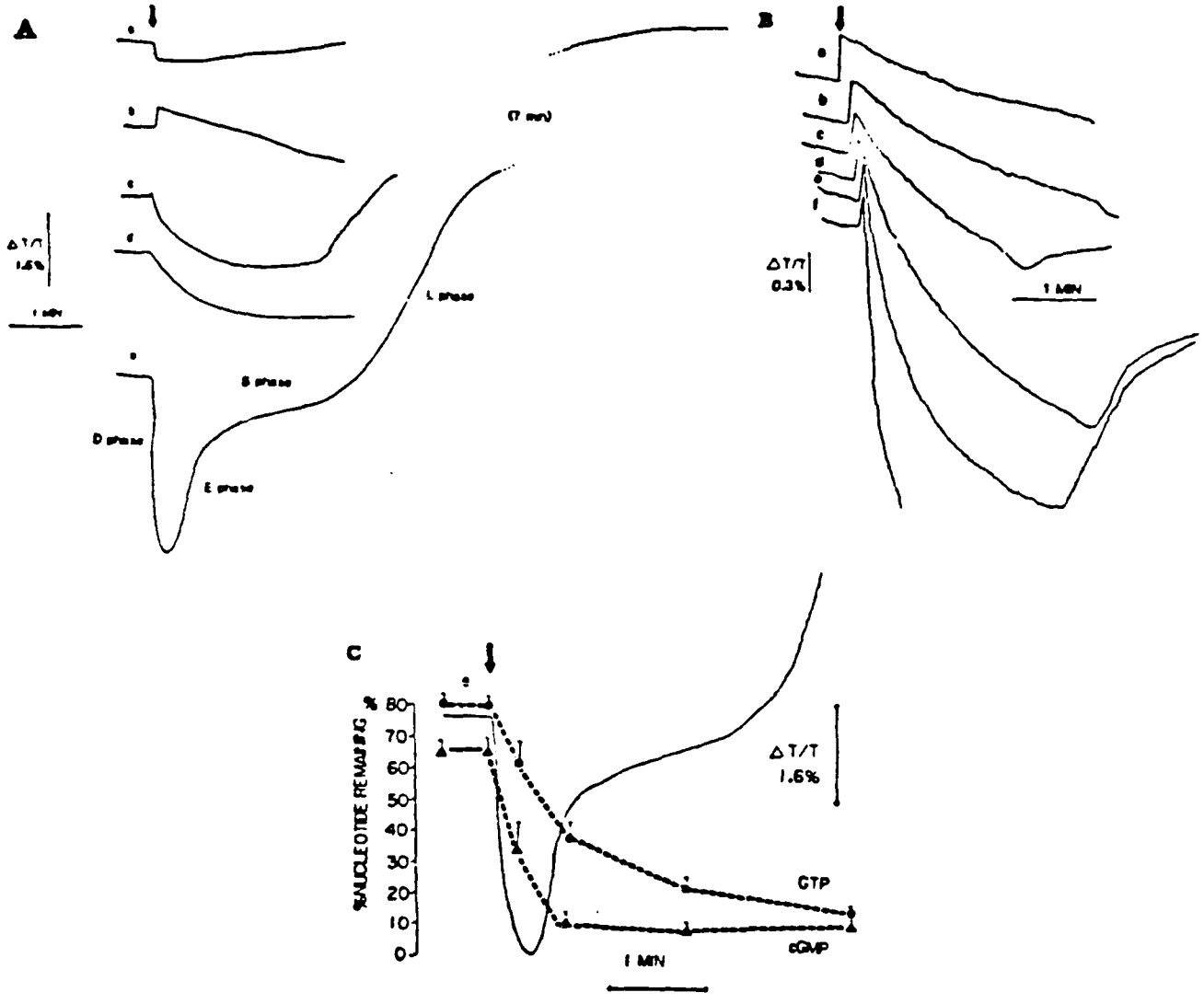

FIGURE 2: (A) Near-infrared (710 nm) light-scattering changes of disk membranes reconstituted with G protein and/or PDE and with different nucleotide composition. [Rhodopsin] = 2 μM. The flash (indicated by the arrow) bleached 2% rhodopsin. Trace a, [G protein] = 200 nM, [PDE] = 60 nM, no GTP. The presence or absence of 1 mM cGMP makes no difference (binding signal; Kuhn et al., 1981). Trace b, [G protein] = 200 nM, no PDE, [GTP] = 3.5 μM, no cGMP (dissociation signal; Kuhn et al., 1981). Trace c, [G protein] = 200 nM, [PDE] = 60 nM, [GTP] = 3.5 μM, no cGMP. Trace d, no added G protein, [PDE] = 60 nM, [GTP] = 3.5 μM, [cGMP] = 1 mM. Trace e, [G protein] = 200 nM, [PDE] = 60 nM, [GTP] = 3.5 μM, [cGMP] = 1 mM. (B) Near-infrared (710 nm) light-scattering changes of disk membranes reconstituted with G protein, GTP, and increasing amounts of PDE. No cGMP present. The flash bleached 0.2% rhodopsin. [Rhodopsin] = 2 μM, [G protein] = 600 nM, and [GTP] = 2.5 μM. Trace a, no PDE; trace b, [PDE] = 20 nM; trace c, [PDE] = 30 nM; trace d, [PDE] = 40 nM; trace e, [PDE] = 60 nM; trace f, [PDE] = 120 nM. (C) Same conditions as (A), trace e; 0.2 μCi of [^{3}H]cGMP and [^{32}P]GTP was present in order to measure PDE and GTPase activities. Every point, mean ± SD of three experiments.

and faster as more PDE was added. The D-phase was further enhanced by the addition of cGMP. The relationship between the signal amplitude and the hydrolysis of added nucleotides is shown in Figure 2C. The rates of hydrolysis did not appear to correlate directly with any of the phases of the cGMP and PDE dependent signal. However, there appeared to be a relationship between the completion of hydrolysis and the onset of the E and L phases, respectively. This relationship was supported by the data in Figures 3A and 4. which show that increasing concentrations of cGMP and GTP delay the onset of the E and L phases, respectively. Figure 3B shows that both 8Br-cGMP and GTPyS (hydrolysis resistant analogs of cGMP and GTP) supported the D-phase of the signal. Thus, it appeared that the energy released by nucleotide hydrolysis was not required to support the underlying process responsible for the light scattering change. The temperature dependence of the light scattering signal is shown in Figure 5. The D-phase was relatively insensitive to temperature, while the E and L phases seemed to be quite temperature sensitive. This result was consistent with the idea that the occurence of these phases required the complete hydrolysis of the requisite nucleotides. The lowest light intensity which elicited the cGMP- and PDE- dependent signal bleached 1/1 $x10^7$ rhodopsin molecules (Figure 6). Figure 7 shows the relationship between light intensity and the kinetics of the D-phase of the signal. The cGMP- and PDE-dependent signal was elicited by bleaching 1/1 x 10^7 rhodopsin molecules. This level of bleaching is about the same as the minimum bleach required for activation of phosphodiesterase.

The cGMP and PDE dependent signal was elicited by addition of nucleotides to bleached membranes in a stirred cuvette. Using this technique, we were able to investigate a variety of different mechanisms relating to the light scattering signal. We have observed that the light scattering signal was reversible if we added 8Br-cGMP and GTP to bleached membranes (Figure 8B). If 8Br-cGMP and GTPyS were used, the transmission decrease was irreversible (Figure 8A). Under the latter conditions, we observed the same membrane suspensions with phase contrast microscopy and noted the appearance of large aggregations of disk vesicles. Negative staining electron microscopy confirmed these observations (Figure 10). We also observed that if GTP was used instead of GTPyS both the transmission change and the vesicle aggregation phenomenon were reversible.

Figure 11 shows the light scattering changes which occured after addition of GTPyS to a suspension of disk membvranes reconstituted with G-protein and PDE in the presence of IBMX (a competitve inhibitor of cGMP hydrolysis). The data show that IBMX substituted for cGMP or 8Br-cGMP. Other competitive inhibitors of cGMP hydrolytic activity also substituted for cGMP. The apparent Km's for the light scattering change (measured as DT/T sec) were IBMX = 85 uM, Theophylline = 330 uM, Aminophylline = 400 uM, Caffeine = 1.5 mM. Occupation of the cGMP binding site by the competitive inhibitor appeared to be sufficient to support the light scattering change. These data support our previous suggestion that nucleotide binding, rather than hydrolysis, is essential for the cGMP and PDE dependent light scattering change.

A number of treatments reversed the nucleotide and enzyme dependent light scattering change. Figure 12 shows that following initiation of the transmission decrease by GTP, addition of EDTA (1 mM final concentration) resulted in a rapid increase in transmission which

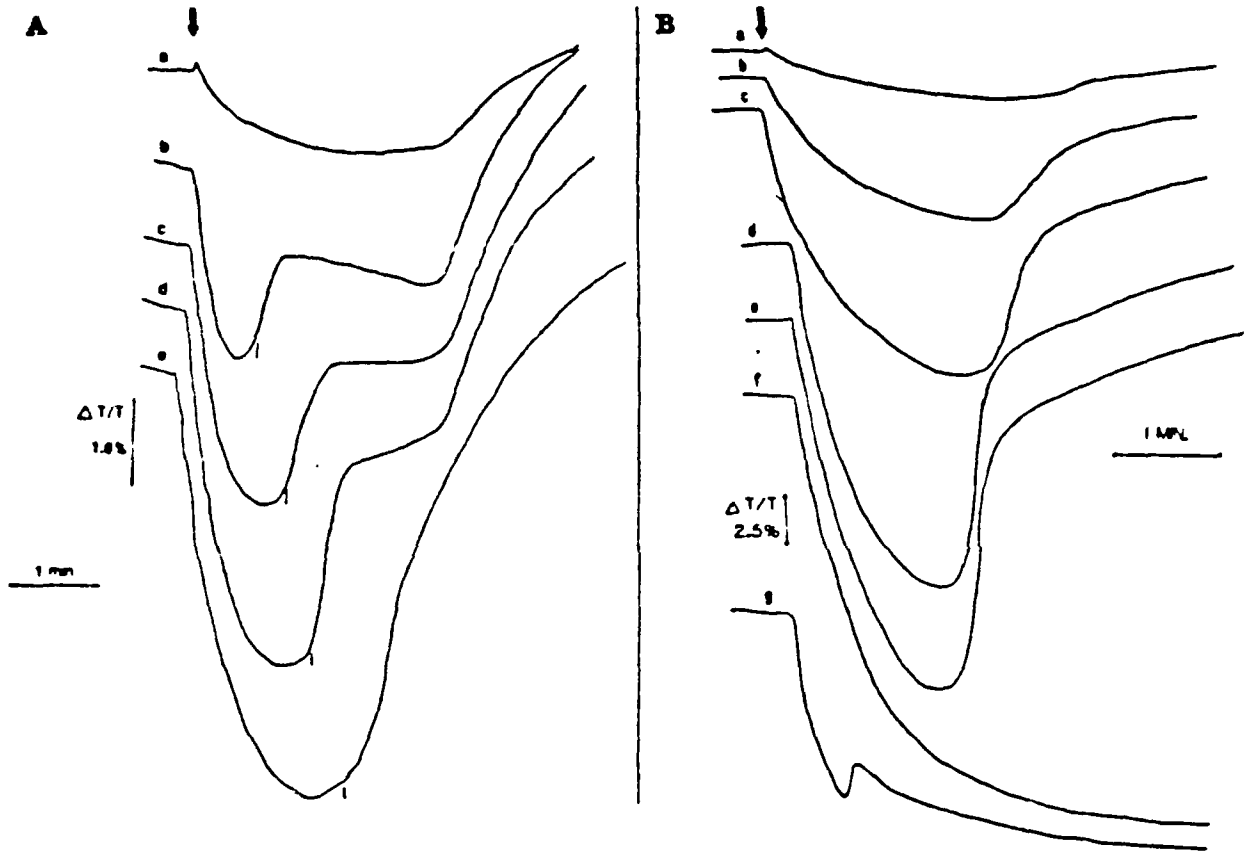

FIGURE 3: (A) Effect of increasing concentrations of cGMP on near-infrared (710 nm) light-scattering changes of disk membranes reconstituted with G protein and PDE. [Rhodopsin] = 2 μM, [G protein] = 600 nM, [PDE] = 60 nM, and [GTP] = 2.5 μM. The flash (indicated by the arrowhead) bleached 0.2% rhodopsin. Trace a, no cGMP; trace b, [cGMP] = 0.5 mM; trace c, [cGMP] = 1 mM; trace d, [cGMP] = 1.5 mM; trace e, [cGMP] = 2 mM. The vertical bars near the traces indicate the time of complete cGMP hydrolysis. (B) Membrane and protein concentrations identical with those in (A). The flash (indicated by the arrowhead) bleached 0.2% rhodopsin. Trace a, [GTP] = 2.5 μM, no cGMP; trace b, [GTP] = 2.5 μM, [8Br-cGMP] = 100 μM; trace c, [GTP] = 2.5 μM, [8Br-cGMP] = 250 μM; trace d, [GTP] = 2.5 μM, [8Br-cGMP] = 500 μM; trace e, [GTP] = 2.5 μM, [8Br-cGMP] = 1 mM; trace f, [GTPγS] = 2.5 μM, [8Br-cGMP] = 1 mM; trace g, [GTPγS] = 2.5 μM, [cGMP] = 1 mM.

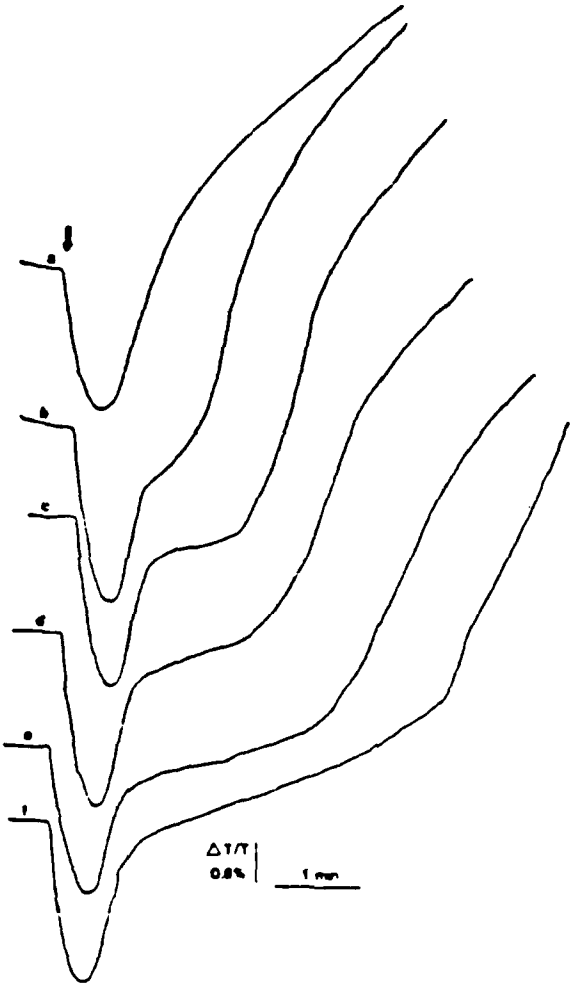

FIGURE 4: Effect of increasing concentrations of GTP on near-infrared (710 nm) light-scattering changes of disk membranes reconstituted with G protein and PDE. [Rhodopsin] = 2 μM, [G protein] = 200 nM, [PDE] = 60 nM, and [cGMP] = 1 mM. The flash (indicated by the arrowhead) bleached 0.2% rhodopsin. Trace a, [GTP] = 1 μM; trace b, [GTP] = 1.8 μM; trace c, [GTP] = 2.5 μM; trace d, [GTP] = 3 μM; trace e, [GTP] = 4 μM; trace f, [GTP] = 5 μM.

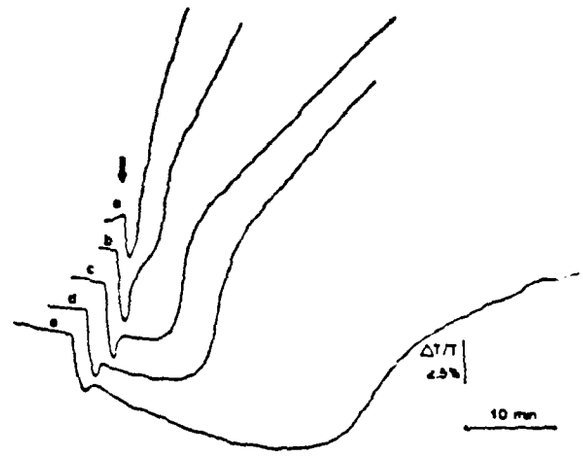

FIGURE 5: Near-infrared (710 nm) light-scattering changes as a function of temperature of disk membranes reconstituted with G protein and PDE. [Rhodopsin] = 2 μM, [G protein] = 200 nM, [PDE] = 60 nM, [GTP] = 2.5 μM, and [cGMP] = 1 mM. The flash bleached 0.2% rhodopsin. Trace a, T = 27.5 °C; trace b, T = 21.5 °C; trace c, T = 14.5 °C; trace d, T = 9.5 °C; trace e, T = 4 °C.

Fig. 6 Light sensitivity of the cGMP and PDE dependent infrared light scattering signal.

Low ionic strength washed toad membranes prepared under infrared light were reconstituted with bovine G and PDE. Final concentrations were Rhodopsin = 5 uM, G = 900 nM, PDE = 100 nM, GTPγS = 5 uM, 8Br-cGMP = 500 uM. Measurement of the scattering signal was performed at 870 nm. Note change in time and transmission scales in various panels.

Trace A : $4/10^{8}$ rhodopsins bleached. Trace B : $1/10^{8}$ rhodopsins bleached. Trace C : $1/10^{8}$ rhodopsins bleached. Trace D : $1/10^{8}$ rhodopsins bleached. Trace E : $1/10^{8}$ rhodopsins bleached. Trace F : $1/10^{7}$ rhodopsins bleached. Trace G : $5/10^{8}$ rhodopsins bleached. Trace H : $2/10^{8}$ rhodopsins bleached.

Fig 7 Plot of the initial speed of DT/TX sec^{-1} against

Fig. 6

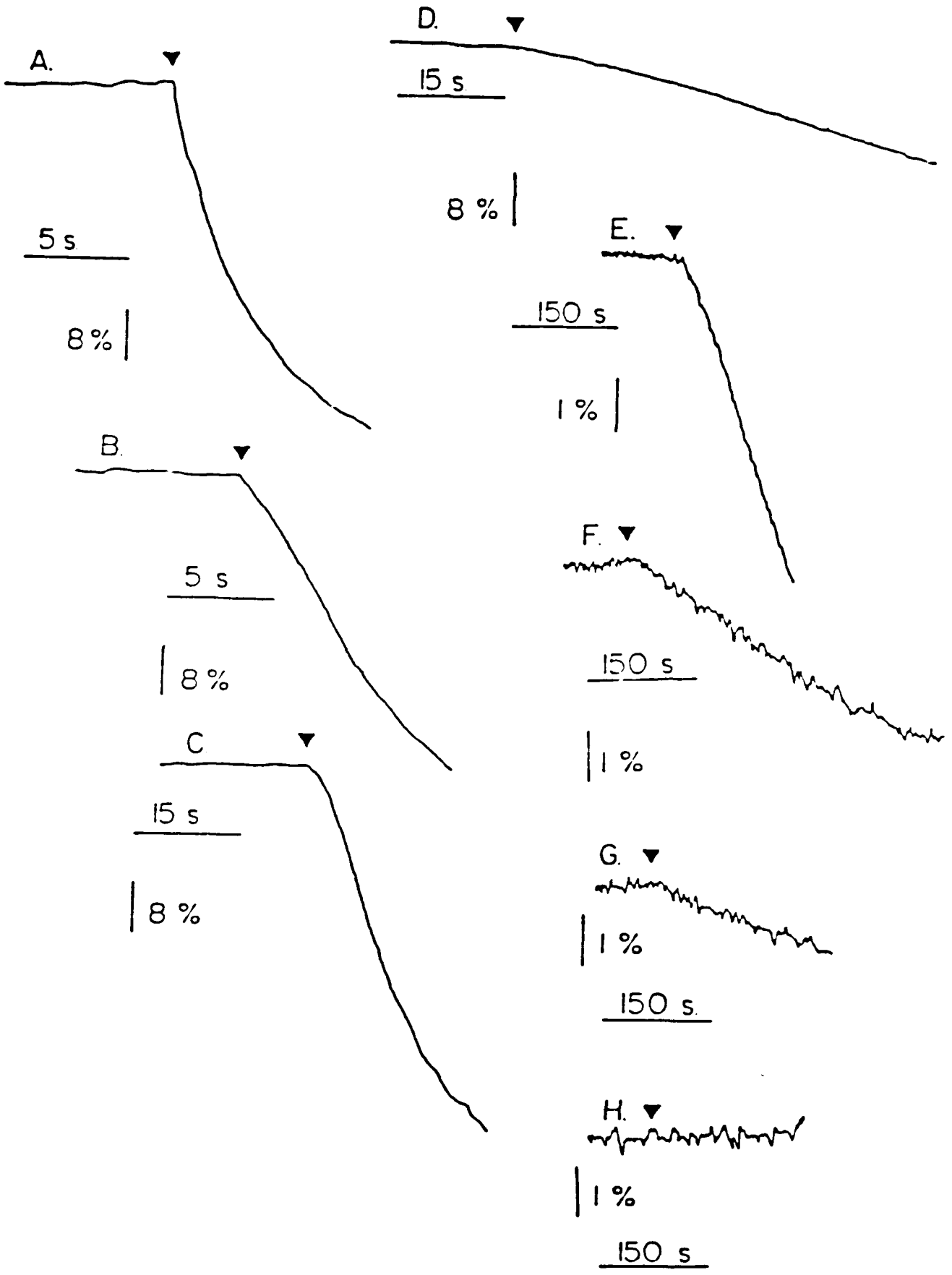

Fig. 7

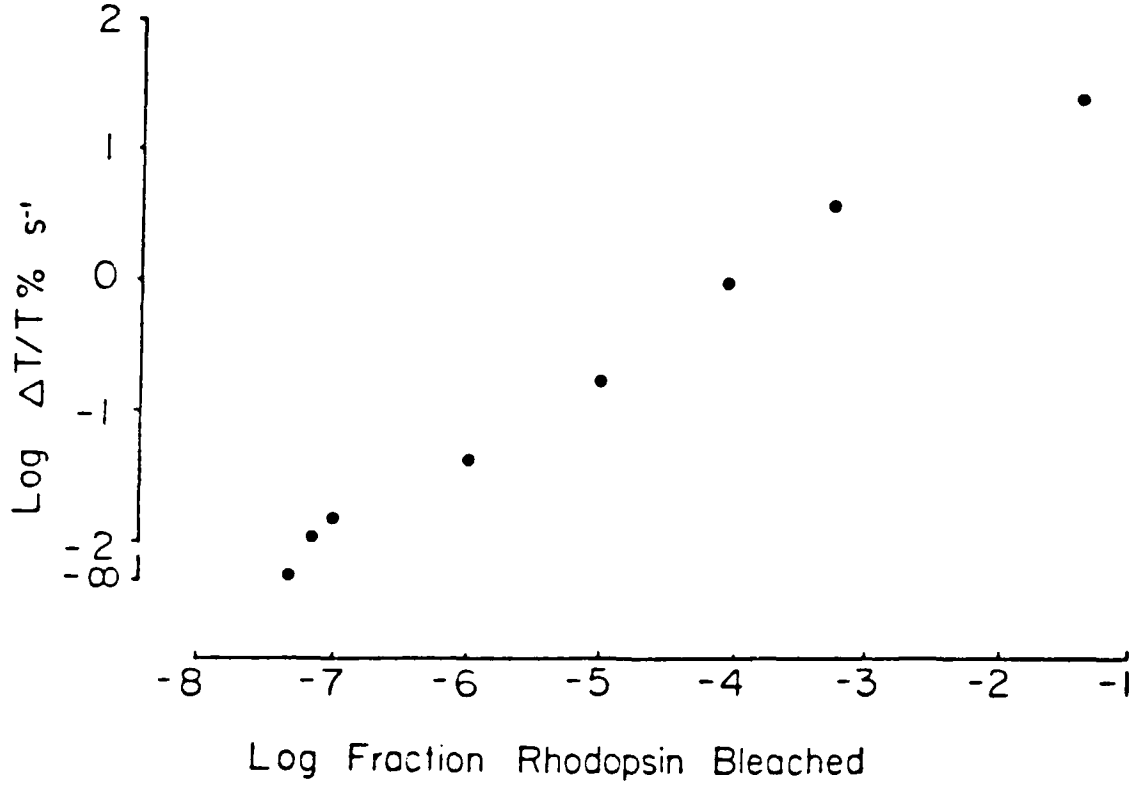

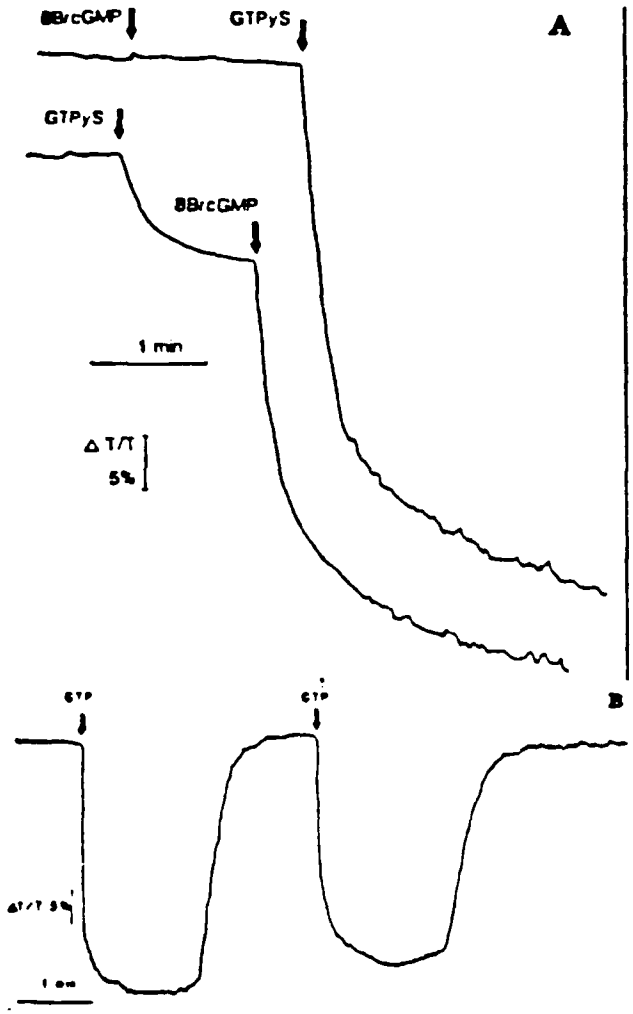

FIGURE 8: Addition of nucleotides to fully bleached disk membranes reconstituted with G protein and PDE: effect on near-infrared light scattering at 710 nm. [Rhodopsin] = 2.5 μM, [G protein] = 200 nM, and [PDE] = 60 nM. Membranes were stirred at 60 rpm. (A) After the addition, [8Br-cGMP] = 1 mM and [GTPγS] = 8 μM. Note that the addition of 8Br-cGMP in the absence of GTPγS is completely ineffective. (B) Effect of repeated GTP additions. After the addition, [GTP] = 5 μM. From the beginning of the experiment, 1 mM 8Br-cGMP is present in the cuvette.

FIGURE 9. Light micrographs of disk membranes reconstituted with G protein and PDE. Bar = 7.5 μM. Both samples were fully bleached. [Rhodopsin] = 2.5 μM, [G protein] = 200 nM, and [PDE] = 80 nM. (A) No nucleotide added; (B) [GTPγS] = 8 μM, [8Br-cGMP] = 1 mM.

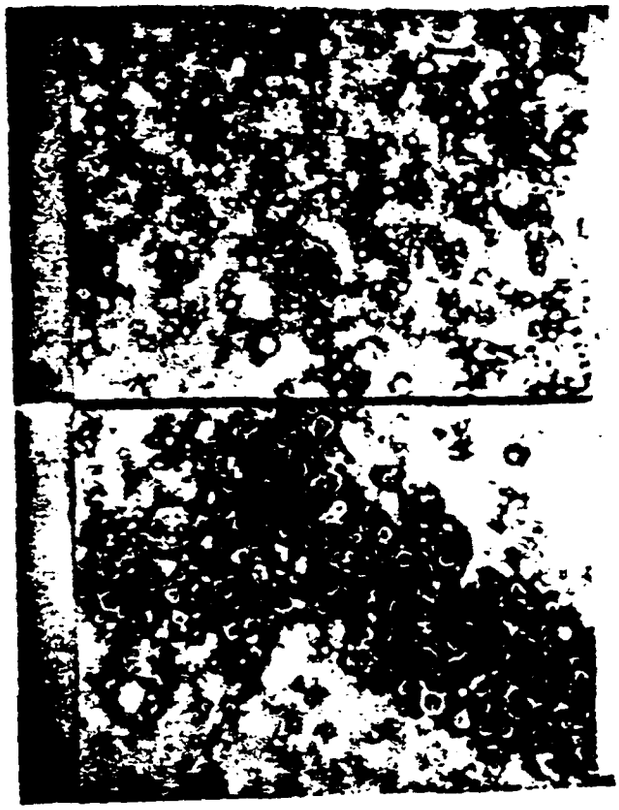

FIGURE 10: Electron micrographs of disk membranes reconstituted with G protein and PDE. Bar = 0.38 μM. Both samples were fully bleached. [Rhodopsin] = 2.5 μM, [G protein] = 200 nM, and [PDE] = 80 nM. (A) No nucleotides added; (B) [GTPγS] = 8 μM, [8Br-cGMP] = 1 mM.

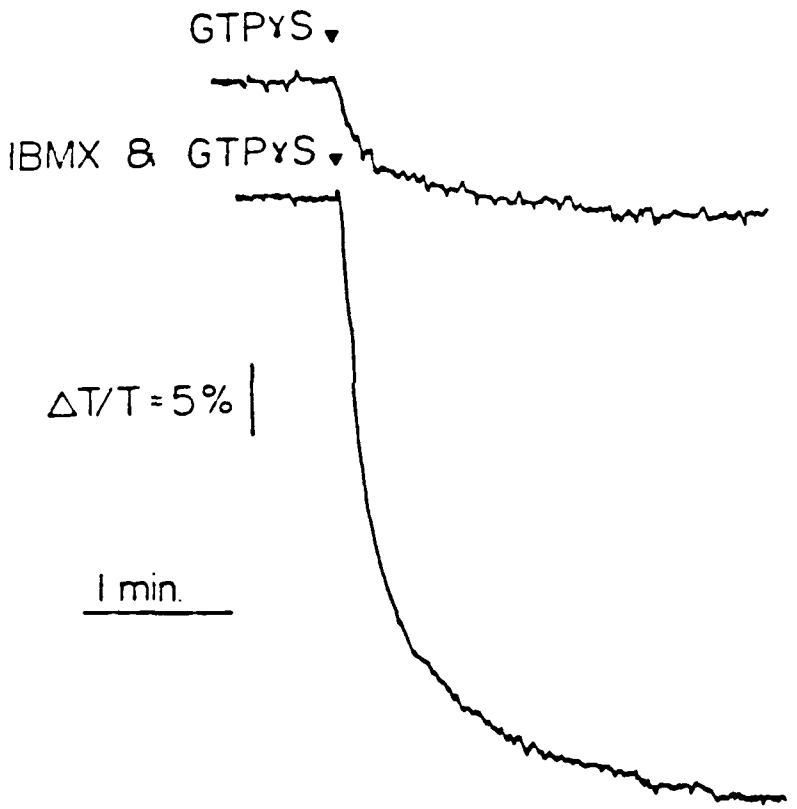

Fig.11 Near infrared light scattering changes (710 nm) of a suspension of fully bleached reconstituted disk membranes. Effect of GTPγS (3 uM) addition in the absence (upper trace) and in the presence (lower trace) of 500 uM IBMX. Rhodopsin = 3 uM, G = 300 nM, PDE = 120 nM.

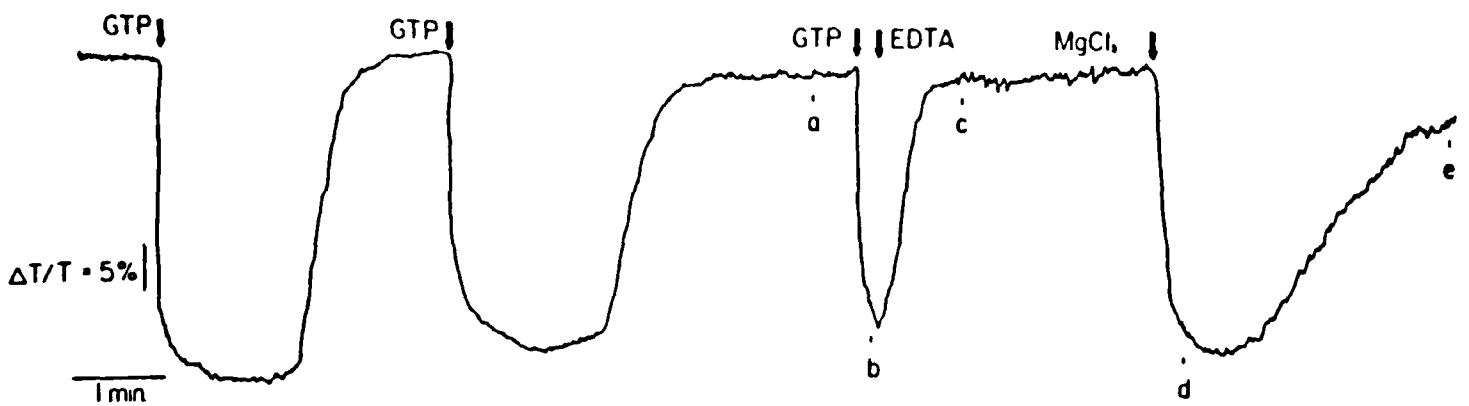

Fig. 12 Effect of EDTA and $MgCl_2$ on the cGMP PDE dependent near infrared light scattering change of a suspension of reconstituted fully bleached disk membranes.

Rhodopsin = 3 uM, B = 300 nM, PDE = 120 nM, BBr-cGMP = 500 uM and $MgCl_2$ = 200 uM present from the beginning. Effect of subsequent addition of GTP (3 uM) EDTA (1 mM) and $MgCl_2$ (3 mM). At the times indicated by the letters samples were collected from the cuvette.

stabilized at the baseline level. Subsequent addition of 3 mM $MgCl_2$ reactivated the transmission decrease. Figure 13, upper trace shows that addition of GTP in the presence of EDTA had no effect on light scattering, but subsequent addition of $MgCl_2$ elicited a large scattering effect. Figure 13, lower trace, shows that addition of $CaCl_2$ or $MgCl_2$ in the presence of EDTA, but in the absence of GTP had no effect on light scattering. Subsequent addition of GTP elicited the usual light scattering change. In all these conditions, the presence of EGTA (a chelator selective for Ca rather than Mg) had no effect on the light scattering changes. From these data, it appears that the cGMP- and PDE-dependent light scattering changes did not result from a charge effect of divalent cations but rather required the presence of Mg (not Ca) as a nucleotide cofactor.

GDP at millimolar concentration, reversed the GTP-dependent activation of the infrared light scattering signal (Figure 14, upper trace). GDP, if added before GTP, prevented the GTP-dependent light scattering decrease. It is interesting to note that GDP did not reverse activation by GTPyS. Similarly colchicine at high concentration (25 mM) was capable of reversing the GTP-dependent decrease in transmission (Figure 15). Lumicolchicine at similar concentrations was also effective. Thus, the effect of colchicine was unlikely to be through its well-documented effect on microtubules or tubulin.

The phosphodiesterase activity in the disk membrane suspensions was measured under the same conditions as those described above for EDTA, GDP, and colchicine (Figure 16). In the presence of these agents, GTP-dependent activation of PDE was completely blocked. In the presence of IBMX, GTP-dependent activation of cGMP hydrolysis by PDE was still present, as was the light scattering signal. The data indicated that GTP-dependent activation of PDE was the trigger for the vesicle aggregation process. The vesicle aggregation/disaggregation processes were the physical mechanism responsible for the light scattering changes. Hence, the light scattering changes reflected the light- and nucleotide-dependent activation of PDE.

We continued our examination of the molecular basis of the infrared light scattering changes in disk membrane suspensions by examining the partitioning of extrinsic membrane proteins between bound and free states during infrared light scattering experiments. We observed that PDE binding increased during the membrane aggregation (decreased light transmission) phase and PDE binding was reduced during the membrane disaggregation (increased light transmission) phase. The results indicated that PDE underwent a light- and nucleotide-dependent binding to disk membranes which correlated with both the aggregation dynamics of disk vesicles and the concurrent light scattering changes.

Figure 17A shows the effect of addition of GTPyS and 8Br-cGMP on light scattering of a suspension of bleached disk membranes reconstituted with G-protein and PDE. As described above, a decrease in infrared light transmission occured after addition of GTPyS. This decrease was further enhanced by addition of 8Br-cGMP. Analysis of protein partitioning (Figure 17B) during this experiment showed that addition of GTPyS decreased PDE in the moderate ionic strength wash (lane b compared with lane a) and increased the amount of PDE released by the low ionic strength wash (lane b' compared with lane a'). Thus, the amount of PDE associated with the membrane (as indicated by the amount released by low ionic strength washing) increased. Upon addition

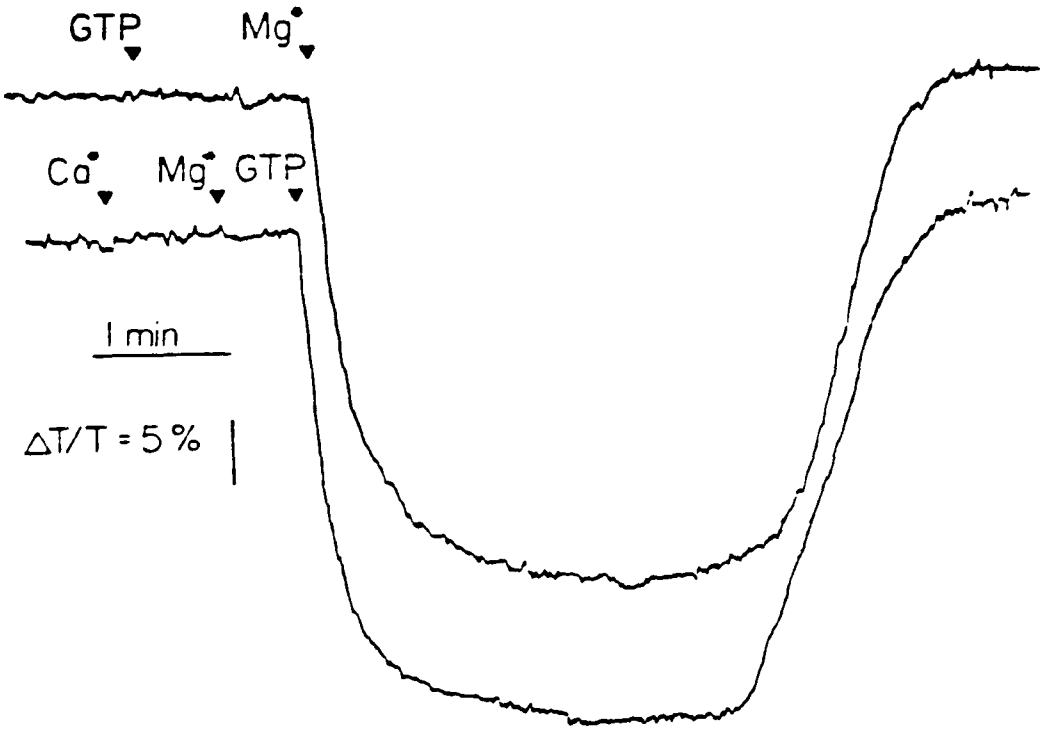

Fig.17 Effect of chelating agents and divalent cations on the cGMP and PDE dependent light scattering changes.
Rhodopsin = 3 uM, B = 300 nM, PDE = 120 nM, 8Br-cGMP = 500 uM, present from the beginning.
Upper trace : EDTA = 200 uM present from the beginning. Effect of subsequent addition of GTP (3 uM) and $MgCl_2$ (1 mM)
Lower trace : EDTA = 200 uM present from the beginning. Effect of subsequent addition of $CaCl_2$ (1 mM), $MgCl_2$ (1 mM) and GTP (3 uM).

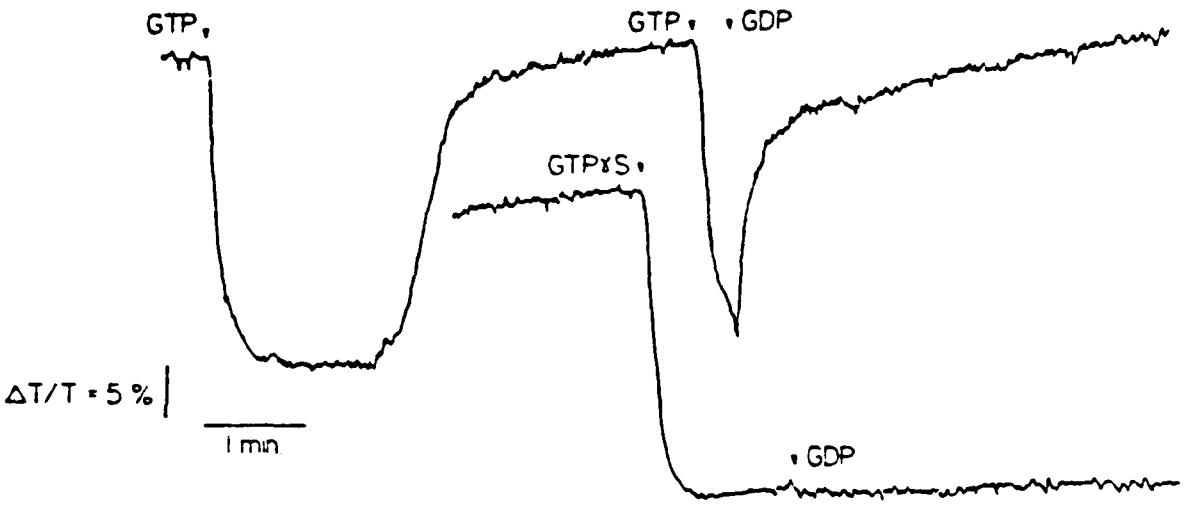

Fig.14 Effect of GDP addition on light scattering changes (710 nm) of a suspension of fully bleached reconstituted membranes. Rhodopsin = 3 uM, G = 300 nM, PDE = 120 nM, 8Br-cGMP = 500 uM, present from the beginning. Upper trace : after addition GTP = 6 uM, GDP = 1.5 mM. Lower trace : After addition : GTPγS = 3 uM, GDP = 1.5 mM.

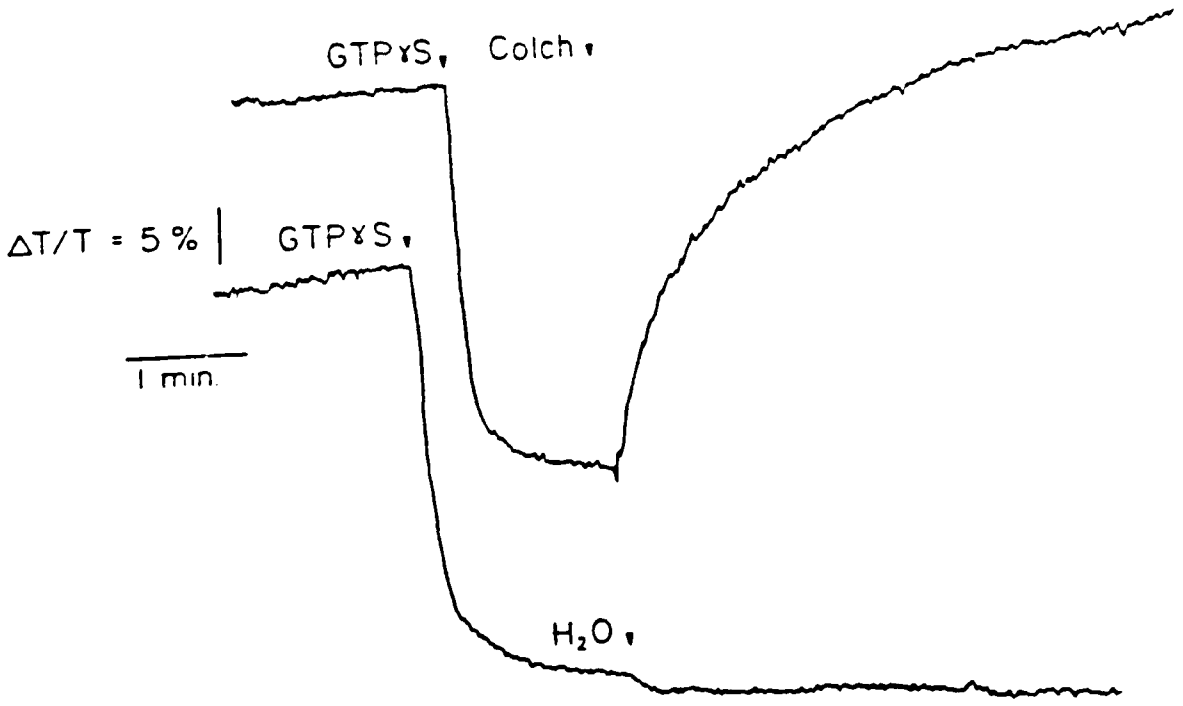

Fig.15 Effect of Colchicine on the cGMP and PDE dependent light scattering changes of a suspension of fully bleached reconstituted disk membranes.
Rhodopsin = 3 uM, G = 300 nM, PDE = 120 nM, 8Br-cGMP 500 uM present from the beginning. After additions GTPγS = 3 uM, Colchicine = 25 mM.

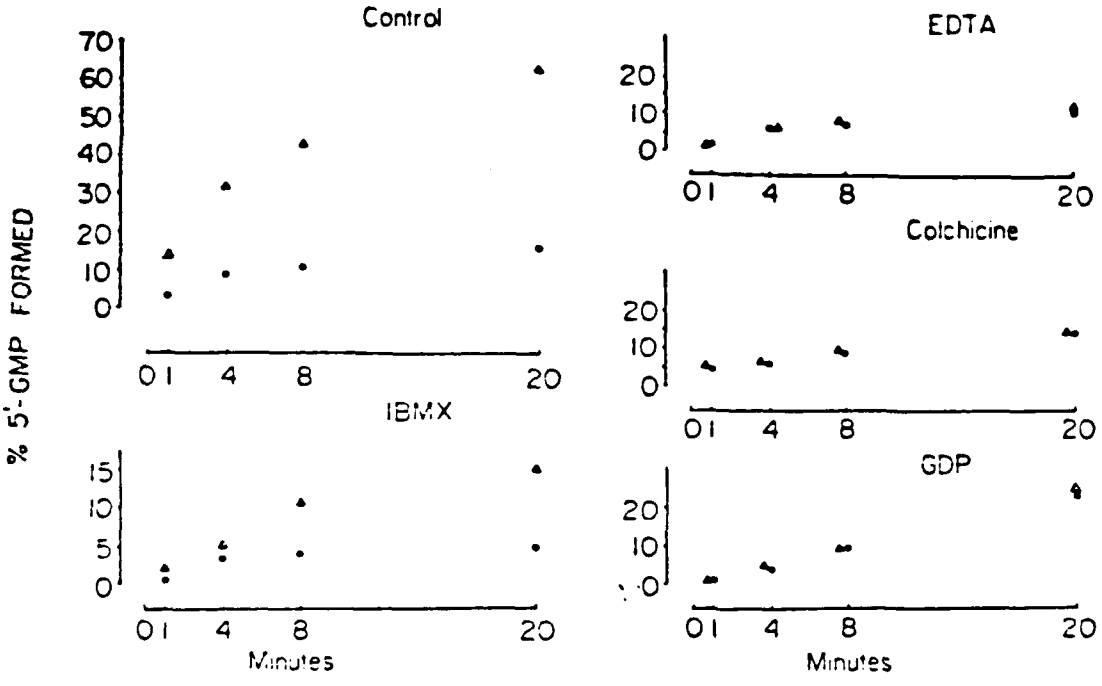

Fig. 16 PDE hydrolytic activity in the presence (empty triangle) and in the absence of GTP (filled circles).

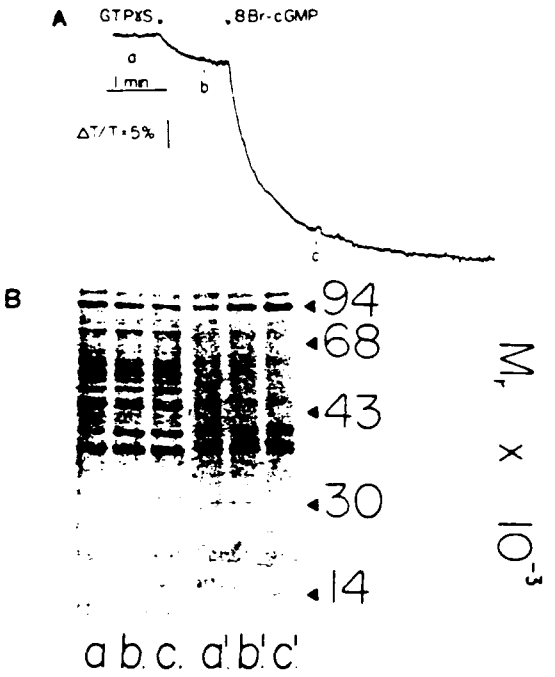

FIGURE 17: Addition of nucleotides to fully bleached reconstituted membranes: effect on near-infrared light scattering at 710 nm. (A) [Rhodopsin] = 2.5 μM, [G protein] = 250 nM, and [PDE] = 100 nM. After the addition, [GTPγS] = 3 μM and [8Br-cGMP] = 500 μM. At the times indicated by a–c, samples were collected from the cuvette and spun at 39000*g* for 4 min. (B) SDS gel showing protein partitioning between moderate and low ionic strength supernatants. Lanes a, b, and c show the moderate ionic strength washes of the samples collected at times a, b, and c, respectively, as indicated in panel A. Lanes a′, b′, and c′ show the proteins extracted by low ionic strength washing of the pellets of the same samples.

of 8Br-cGMP, a further increase in binding to the membrane occured (Figure 17B, lane c' compared with b').

Addition of GTP to bleached disk membranes, reconstituted with PDE, G-protein, and 8Br-cGMP resulted in a large reversible decrease in light transmission (light scattering increase) (Figure 18A). The light scattering change was reversible since the signal level returned to baseline. A subsequent addition of GTPyS produced an irreversible transmission decrease. In other experiments (data not shown), up to 4 additions of GTP were capable of eliciting transmission decreases of similar amplitude. Figure 18B shows the distribution of proteins between moderate and low ionic strength fractions obtained from aliquots of the disk membrane suspensions sampled from the cuvette during the scattering experiments. Before the addition of GTP(Figure 18B), a small amount of PDE was present in the low ionic strength wash (lane a'), while most PDE was present in the moderate ionic strength wash (lane a). After addition of GTP (Figure 18B), most PDE was present in the low ionic strength wash (lane b') and only a small amount was present in the moderate ionic strength fraction (lane b). When the scattering signal was again at its baseline level, the original distribution of PDE was restored (Figure 18B, lanes c and c'). After addition of GTPyS (Figure 18B), the amount of PDE increased in the low ionic strength fraction (lane d') and a reduced amount was present in the moderate ionic strength fraction (lane d).

Figure 18C shows the state of vesicle aggregation under identical experimental conditions. It is clear that when the vesicles were in the aggregated state, an increasing population of PDE molecules were bound to the disk membrane. When the vesicles disaggregated, the PDE molecules reapppeared in the moderate ionic strength fraction. Thus, it appears likely that PDE binding and release may be related to vesicle aggregation and to the nucleotide and enzyme dependent light scattering changes in these membrane suspensions.

The data presented above show that light and nucleotide affect PDE binding to disk membranes. Under conditions which enhance PDE binding to the membrane, G-protein is released from the membrane. It appears that under these experimental conditions only G-protein and PDE are changing their association with the membrane. Thus, increased PDE binding is not merely a consequence of the membrane aggregation process which occurs under the same conditions. A simple explanation of these phenomena would be that PDE release from the membrane is diminished by aspects of the vesicle aggregation, e.g. decrease in exposed membrane surface area or mechanical trapping of protein, etc. However, careful examination of the gels shows that while many other proteins are present in our partially purified extracts, only G-protein and PDE undergo nucleotide dependent binding and release. It is also possible that there is competition between G-protein and PDE for a binding site on the disk membrane. As G-protein binding is decreased (by GTP addition) PDE binding could increase. However, increasing the ratio of G-protein to PDE in the reconstitution mixture does not decrease PDE binding as would be expected if there were competition for a common binding site (data not shown). Since addition of GTP (or its hydrolysis resistant analogs) in the presence of G-protein activates PDE, it seems likely that this activation may alter the conformation of PDE so that its affinity for its membrane binding site is increased. While this seems to be the most promising interpretation of the data, we can not

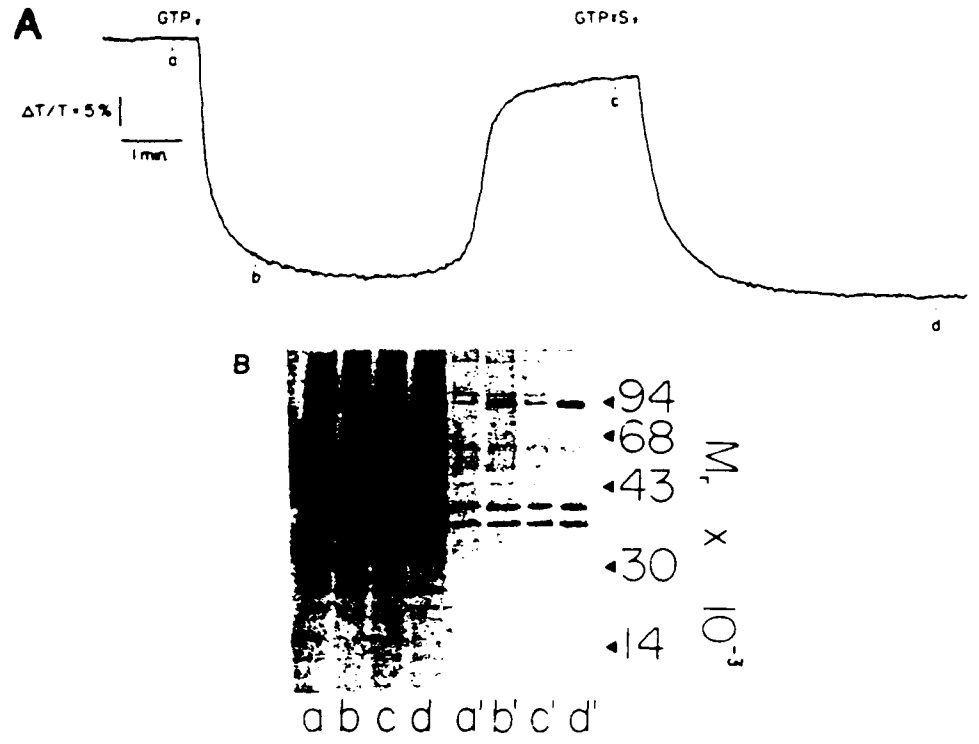

FIGURE 1: Addition of GTP (5 μM) and GTPγS (3 μM) to fully bleached reconstituted membranes: effect on near-infrared light scattering at 710 nm. (A) [Rhodopsin] = 3 μM, [G protein] = 300 nM, [PDE] = 120 nM, and [8Br-cGMP] = 500 μM. At the times indicated by a–d, samples were collected from the cuvette. (B) Protein partitioning between moderate and low ionic strength supernatants. Lanes a, b, c, and d show the moderate ionic strength supernatant of the samples collected at times a, b, c, and d, respectively, as indicated in panel A. Lanes a', b', c', and d' show the proteins extracted by low ionic strength washing of the pellet of the same samples. (C) Phase-contrast light micrographs of the samples collected at times a–d. Bar = 5 μM for all the samples.

yet define the mechanism for the increase in PDE affinity for the membrane in these experiments.

We have been unable to observe light- and nucleotide-dependent binding in disrupted, unwashed ROS membranes. The light- and nucleotide-dependent light scattering signal is present in these membranes, but it is extremely small compared to the signal in the reconstituted system. If, in native membranes, there is a high ratio of PDE binding sites to PDE, then most of the PDE will be bound and the change in PDE binding will be difficult to detect. We believe that increasing PDE concentration makes it possible to observe the PDE binding/release phenomenon which is present, but not normally detectable, in native membranes or intact rod outer segments.

The physical basis of the PDE- and nucleotide-dependent infrared light scattering signal reported here appears to be vesicle aggregation/disaggregation. The data suggest that GTP-dependent activation of PDE results in enhanced PDE binding to the disk membrane under our experimental conditions. PDE inactivation which occurs after completion of GTP hydrolysis may release PDE from the membrane. We believe that the changes in PDE binding/release are related to vesicle aggregation/disaggregation. Therefore, we propose that the changes in near infrared light scattering observed in these experiments reflect PDE activation/inactivation. A similar relationship between PDE activation and near infrared light scattering changes has been proposed by Kamps et al.(1985) based on studies of permeabilized rod outer segments.

Harari, Pinto, and Brown, 1978 described a near infrared light scattering signal in the isolated, superfused retina of the toad. According to their report, this signal had its origin in the outer segment of the rod photoreceptor. We wished to determine if there was a relationship to the cGMP- and PDE-dependent light scattering signal <u>in vitro</u> and the signal in the retina. Figure 19 shows scattering signals recorded from the isolated toad retina. The waveform increased in complexity as the intensity of the light stimulus was increased. The two slower components of the signal which appeared at higher light intensities were not evident in the report of Harari et al. Figure 17 also shows that the PDE inhibitor, IBMX had a profound effect on the waveform and kinetics of the latter two phases of the scattering response. In fact, these components were seen at lower flash intensities in the presence of the inhibitor. The rapid phase of the scattering response seemed relatively insensitive to IBMX. Figure 20 shows that the effect of IBMX was reversible. MB22968, another PDE inhibitor, also produced a similar effect on the light scattering response (data not shown). We believe these experiments indicate that there is a relationship between the <u>in vitro</u> and <u>in vivo</u> signals since these drugs are reported to change the level of cGMP in the rod.

Figure 21 shows that after application of dinitrophenol and 2-deoxyglucose (a treatment which will lower the nucleotide concentrations in the rod) the scattering signal decayed. The first effect of this treatment was to block the slow phase of the scattering change. With time, the initial rapid phase appeared to be isolated until it finally decayed and the entire signal was lost. The rapid signal in the retina appears similar to the 'dissociation signal' recorded from rod outer segments, which has its origin in the GTP-induced release of G-protein from the disk membrane. Since rod

Fig. 19

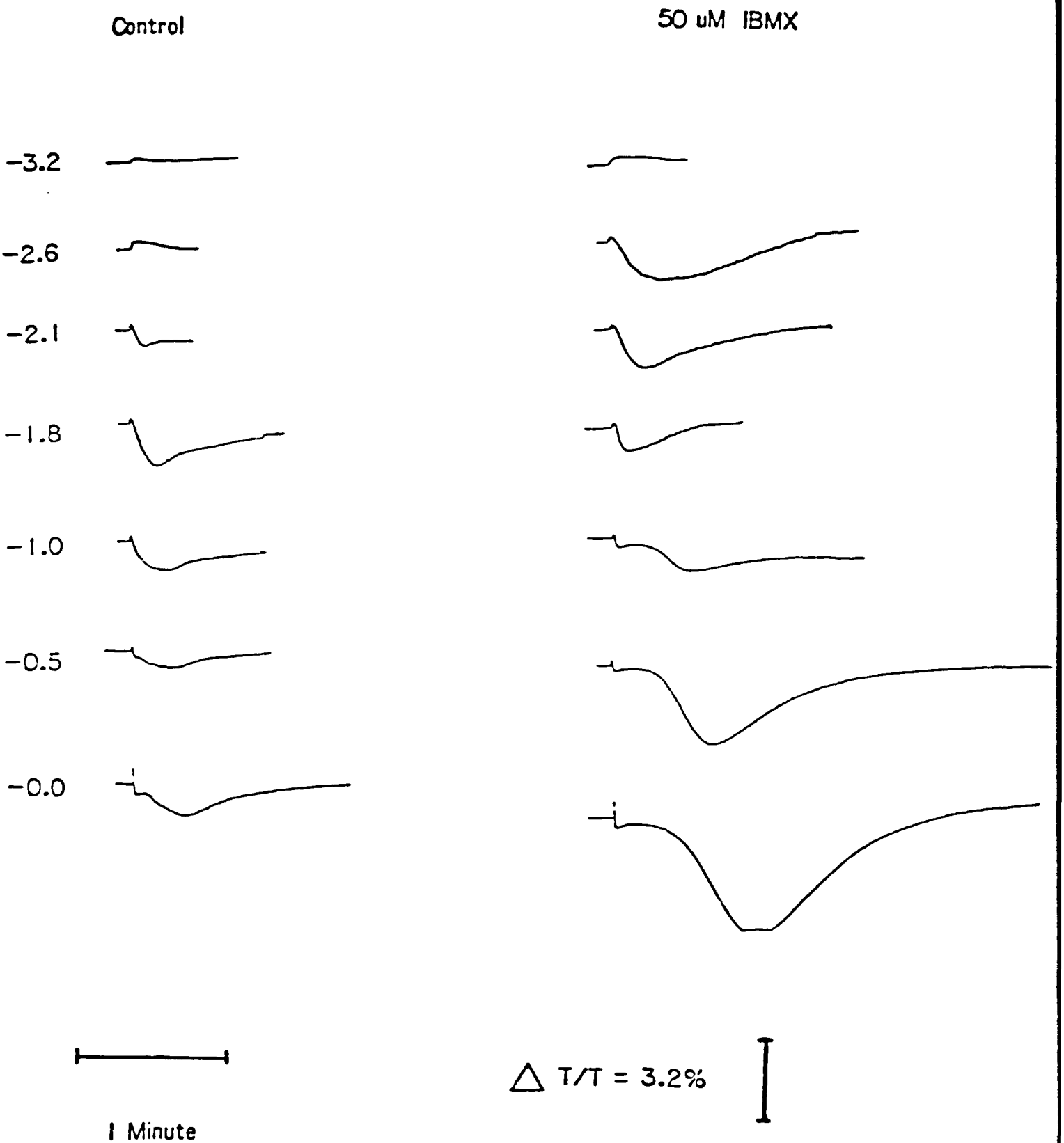

Fig. 20

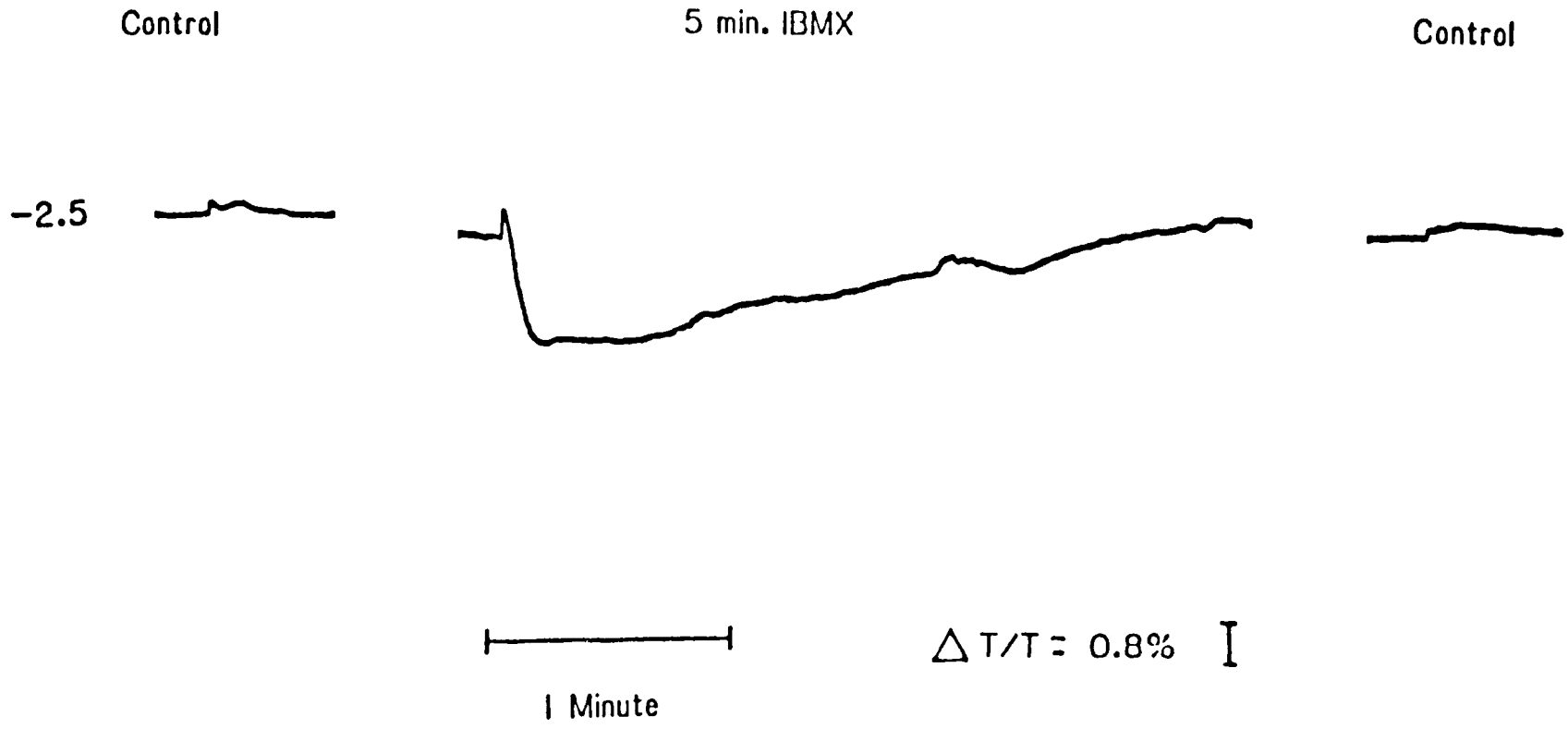

Fig. 21

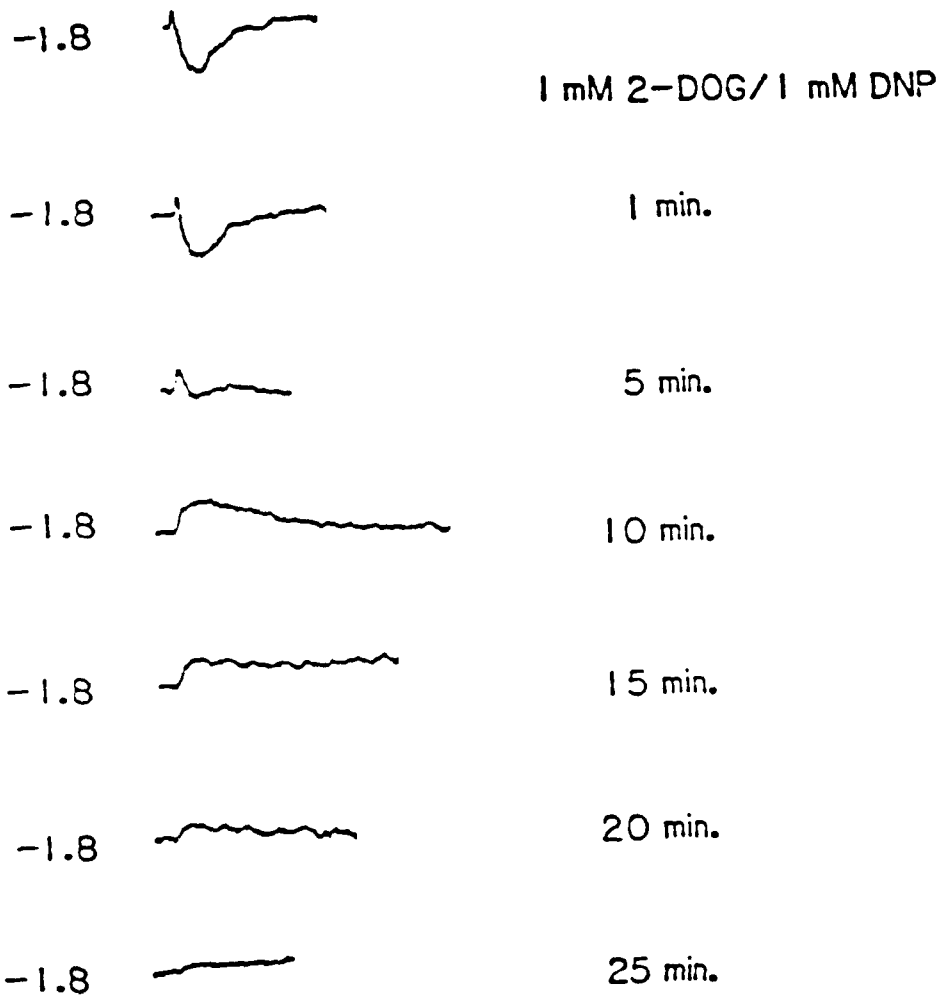
-1.8
1 mM 2-DOG/1 mM DNP
-1.8
1 min.
-1.8
5 min.
-1.8
10 min.
-1.8
15 min.
-1.8
20 min.
-1.8
25 min.
1 Minute
ΔT/T = 0.8%

photoreceptors contain millimolar concentration of GTP and micromolar concentration of cGMP, the changes in the scattering signal would be readily explained if cGMP depletion occured before GTP depletion. Thus, in the absence of cGMP the component of the signal which corresponded to the in vitro cGMP and PDE signal was eliminated. The signal which remained corresponded to the G-protein 'dissociation' signal. As GTP was depleted, this aspect of the signal was lost. More definitive experiments are necessary to confirm this interpretation.

The plasma membrane of the rod outer segment of rod photoreceptors contains a cGMP-modulated cation conductance. This conductance is thought to be involved in phototransduction. While two polypeptides which mediate cGMP-activated cation fluxes when reconstituted into liposomes have been identified (Matesic and Liebman, 1987; Cook et al., 1987), the identity of the light-sensitive conductance remains a mystery. We report here recordings of cGMP-activated single channel currents observed in patches excised from phospholipid vesicles containing purified (>99%) bovine opsin. Two elementary conductances, of 32 and 17 pS, were observed in the presence of 10-200 uM cGMP. Both individual channel openings (mean open times, 1.6 ms for the 32 pS conductance and 1.0 ms for the 17 pS conductance) and bursts of openings (mean burst duration 2-3 ms for large events) were observed. The cGMP-activated channel activity could be observed in the presence or absence of Ca^{2+}. These results suggest that rhodopsin, in addition to performing as the receptor in the rod, is the light sensitive pore as well.

Figure 22 shows the silver-stained SDS electrophoretic pattern of stripped bovine rod outer segment membranes (lane a) and the purified (>99%) opsin contained in the phospholipid vesicles used for the patch-clamp experiments (lane b). A dimer (64 kd) of the 37,000 kd opsin monomer is faintly visible (Fig. 22, lane b). Immunoblots using a polyclonal anti-rhodopsin antibody showed staining patterns identical to those observed in Coomassie-stained gels of opsin (i.e. identical monomer/dimer etc. staining ratios; data not shown). Figure22, lane c shows the polypeptide(s) purified by the method of Cook et al., which is thought to mediate cGMP-activated cation fluxes. In this Laemmli gradient gel system their partially purified protein migrated with an apparent molecular weight of 54 kd. Figure 22, lane d shows purified opsin to which the protein(s) shown in lane c were added.

Figure 23 shows the current recorded from a patch excised from an opsin-phospholipid vesicle and held at +60m mV. In the absence of cGMP, or in the presence of 1 uM cGMP no significant current fluctuations were observed. Addition of 10 uM cGMP resulted in current fluctuations which resembled individual ion channel events. The most easily observed events had a mean amplitude of 1.9 pA, corresponding to a conductance of 32 pS. These were sometimes accompanied by smaller events, events with a mean current amplitude of 1.0 pA (conductance 17 pS), roughly one-half that of the large events (see Figure 25). Removal of cGMP resulted in a cessation of the fluctuations, showing that they were not the result of seal breakdown. Addition of increasing (100-200) concentrations of cGMP caused a reversible increase in the frequency of single channel events, leading to stacked events, longer bursts, and summing to give noisy currents, many times the magnitude of that characterized by a single event. The normalized dose-response relation for three patches analyzed was well fit by the Hill equation, giving

Fig. 22 Silver-stained SDS 6-12% Laemmli[9] polyacrylamide gel of stripped bovine rod outer segment membranes (a), phospholipid vesicles containing purified bovine opsin (b), protein isolated according to the method of Cook et al. (c),[5] and purified opsin combined with Cook protein (d). All lanes are from the same gel. The opsin was determined to be >99% pure by gel densitometry of Coomassie-stained gels(data not shown).
Methods. Stripped bovine outer segment membranes from 200 fresh calf eyes were solubilized in 18 mM CHAPS, 100 mM NaCl, 0.5 mM $CaCl_2$, 10 mM Tris, 5 mM DTT, pH 7.4, containing 1.0 mg ml^{-1} (Buffer A) and centrifuged at 39,000 g for 30 min. The supernatant was loaded onto a Con-A Sepharose column (1.6 x 20 cm, Pharmacia) and washed with Buffer A. Pure opsin was then eluted with Buffer A containing 0.5 M 1-O-methyl α-D-glucopyranoside.[7] Fractions containing opsin were dialysed against 100 mM NaCl, 0.5 mM $CaCl_2$, 10 mM Tris, 5 mM DTT, pH 7.4 (Buffer B) and the resulting opsin-phospholipid vesicles were centrifuged at 15,000 g, resuspended in 100 ml of Buffer B, and centrifuged three more times. Vesicles were resuspended in Buffer B, aliquotted, and stored at -80°C. Freeze-Thaw-Liposomes (FTLs) containing opsin were prepared by sonicating a mixture of phosphatidyl ethanolamine (PE), phosphatidyl serine (PS), and phosphatidyl choline (PC) at a ratio of 5:2:3, respectively, in Buffer C at a concentration of 20 mg ml^{-1}, adding opsin-PC vesicles and quickly freezing the aliquotted suspension.[10] Aliquots were stored at -80°C and thawed just before use. Patch experiments were performed in visible light at room temperature (22-25°C). The phospholipid:opsin molar ratio (600:1) was determined by gel densitometry and confirmed by regeneration to isorhodopsin with 9-cis-retinal and analysis by difference spectrophotometry (A_{280}/A_{498} = 1.5). The estimate of number of (properly oriented) opsins per patch assumes a 10 Å diameter for each phospholipid pair, giving ~1.3 X 10^5 phospholipid pairs per 0.4 μm diameter patch. Assuming that 50% of the opsin molecules are correctly oriented and correcting for the surface area contribution of the opsin, approximately 200 opsin molecules should be contained in each patch at the above lipid:opsin ratio.

Figure 22

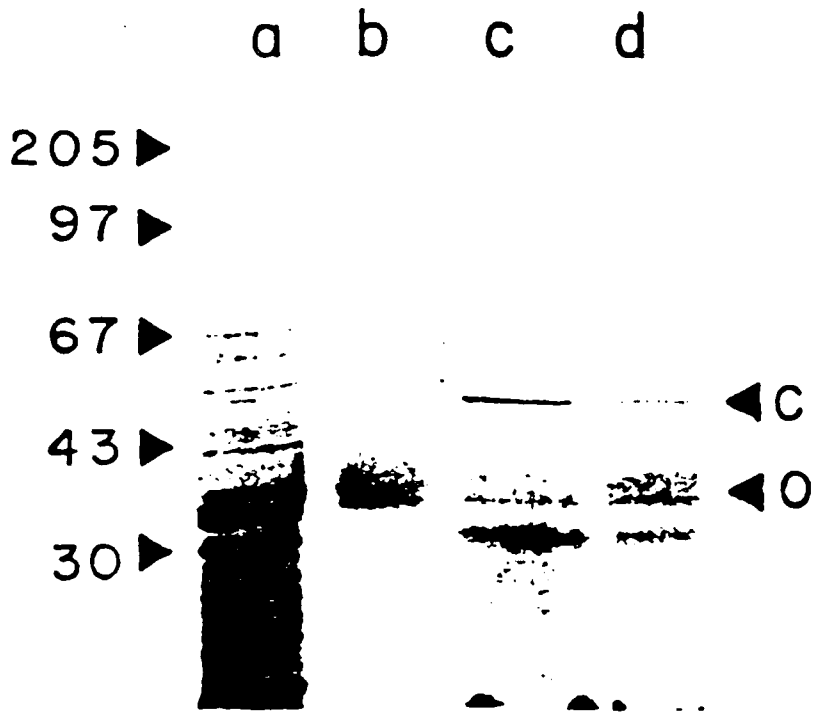

Fig 23 cGMP-activated single channels recorded from a patch excised from an opsin-phospholipid vesicle during application of cGMP in the bath solution. Isotonic solution (150 mM NaCl, 0.5 mM $CaCl_2$, 10 mM Tris, 1 mM DTT, pH 7.4; Buffer C) was present on both sides of the patch. Calibration bars to the right of each trace represent $\pm$2 pA. Traces are (non-continuous) 313 msec records taken from a continuous experiment. Holding potential was +60 mV (pipette negative). All records were low-pass filtered at 2 kHz. In this experiment 50 µM cAMP was applied to the patch between the control (trace 8) and the application of 100 µM cGMP (trace 9). The cAMP did not activate single channel activity (data not shown). Phospholipid:opsin molar ratio in this patch was 600:1. Methods. The fire-polished patch pipettes, containing Buffer C, were made from 1.2 mm I.D. thick-walled borosilicate glass capillaries and had lumens of $\leq$ 0.4 µm. The exterior of the pipette was coated with Sylgard to reduce electrical noise. About 1 µl of the FTL suspension was layered onto the bottom of a 250 µl chamber containing Buffer C.[10,11] The chamber was mounted on an inverted microsope (Zeiss Invertoscope D) and gigaohm seals were made on an FTL. The patch was excised by a gentle tap on the micromanipulator used to position the pipette. The pipette was then passed through the Buffer-air interface to ensure that if a vesicle was formed it was disrupted.[12] Seal resistances ranged from 30 to 300 gigaOhm. Current was measured with a WPI S-7450 patch amplifier in the voltage-clamp mode. The current and clamped voltage were stored on analog tape and subsequently digitized for analysis.

Figure 23

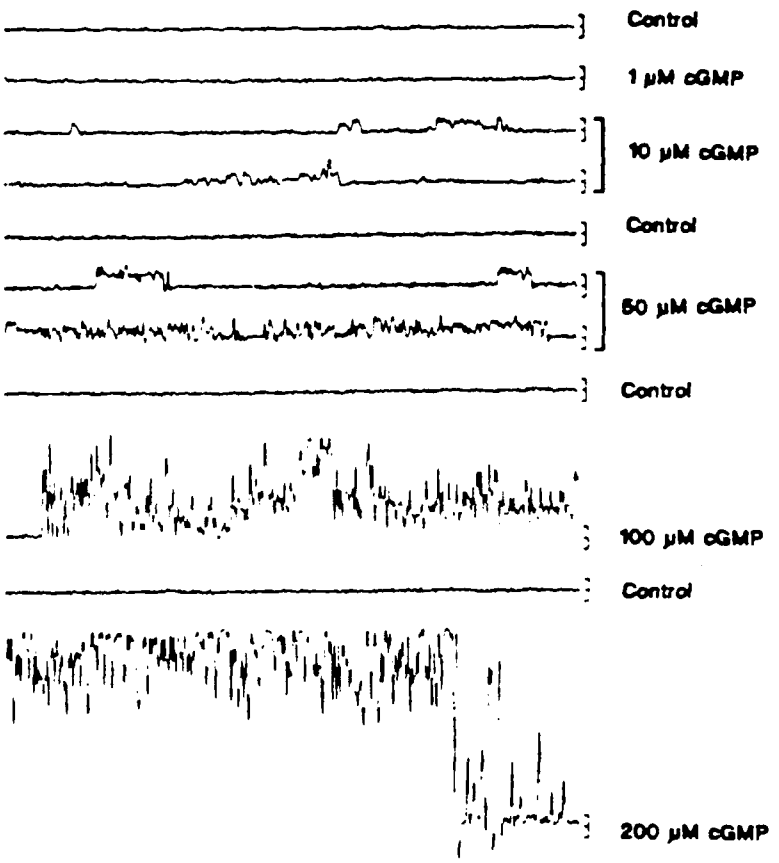
Control
1 μM cGMP
10 μM cGMP
Control
50 μM cGMP
Control
100 μM cGMP
Control
200 μM cGMP

slopes of 1.7-1.9 and $K_{1/2}$ of 30-45 uM (data not shown). The apparent unit conductance, a, calculated from the slope of the relation between the mean current, r, and the variance, s^2, for five patches was 2.0$\pm$ 0.2 pA at 60 mV (See Fig. 23, legend). Saturating current for those patches at 200 uM cGMP was 35$\pm$6 pA. Taking the single channel current to be 1.9 pA, the number of channels conducting current for 50% of the time in a typical patch can be estimated as 37. Alternatively, there could be 70 channels per patch if the small unit conductance is assumed. The number of properly oriented opsin molecules contained in these patches was estimated to be 200 from gel densitometry and spectrophotometric analysis of isorhodopsin regenerated by adding 9-cis-retinal to opsin/phospholipid vesicles (See Figure 22, legend). In order to account for the number of observed channels, a contaminant protein would have to constitute at least 19% of the total protein in the purified opsin. Three patches excised from vesicles containing 9 times less opsin/phospholipid (22 opsin molecules per patch) had saturating currents of 8$\pm$ pA, corresponding to an estimated 8 channels per patch for the large unitary events. This would require an even larger (40%) contamination to account for the channel activity observed.

Figure 24 summarizes the amplitude and kinetic distributions of channel activity elicited by 50 uM cGMP from the experiment in Figure 23. Figure 23a compares the current amplitude distribution observed in the presence of cGMP (open squares) with that observed in the absence of cGMP (open circles). The control plot was scaled to the same height as the zero centered peak of the cGMP plot. The cGMP plot, in addition to a peak centered at zero, has another peak of mean amplitude 1.9 pA. This appears to correspond to the ampitude of the large unitary events. Figure 23b and 23c analyze the open times and burst times of events selected by a window of 1.4-2.5 pA. The open times of the events were exponentially distributed and had a time constant of 1.6 ms (uncorrected for 2 kHz filtering). The burst durations were also roughly exponentially distributed, with a time constant of 2.6ms. These time constants are similar to those observed by Haynes et al. for the kinetics of cGMP-activated single channel events in patches excised from the plasma membrane of amphibian rod outer segments. Analysis of amplitude and kinetics of data from five other patches gave similar meann unit amplitudes (1.9-2.4 pA) as well as open time and burst time constants (mean open time 1.2-2.4 ms, burst durations of 1.9-3.5 ms). Analysis of 50 uM cGMP-activated channel activity from three patches in low divalent solutions (150 mM NaCl, 0.1 mM EDTA, 0.1 mM EGTA, 10 mM Tris, 1 mM DTT) yielded comparable amplitude (1.9-2.5 pA) and kinetic (mean open time 1.4-1.6 ms, burst duration 2.1-3.4 ms) parameters. Indeed, the only apparent effect of Ca^{2+} on patches was to increase the likelihood and stability of seals. Thus, its inclusion in most experiments.

Accompanying the more prominent 32 pS events were smaller events usually observed at low cGMP concentrations. Figure 25a shows a burst of these small events elicited by addition of 10 uM cGMP. Figure 25b compares the current amplitude plot of this burst (open squares) with that of a control plot (open circles). The non-zero peak has an apparent mean of 1.0 pA, corresponding to a unit conductance of 17 pS; the plot generated by the difference of the cGMP and control plots could be fitted with a gaussian with mean of 1.0 pA and standard

Fig. 24 Analysis of the experiment shown in Fig. 2. a, Current probability function of multiple records obtained in the absence (circles) and presence of 50 μM cGMP (squares). The data were obtained from 20 s records of 40,000 points each. The control plot was fitted by a gaussian distribution with mean of 0 pA and standard deviation of 0.15 pA. The plot taken from the difference between the control and cGMP plots (not shown) could be fit by a gaussian with a mean of 1.9 pA and a standard deviation of 0.31 pA. b, Plot of open times for events with amplitudes between 1.4 and 2.5 pA for the same 50 μM cGMP record described above. Events for open times of less than 1 ms were not included to minimize artifact due to 2 kHz filtering. The solid line is a single exponential with time coure 1.6 ms fit to the open time data. c, Plot of burst durations for the large events (between 1.4 and 2.5 pA). A burst was defined as a single-channel opening or a collection of consecutive openings separated by closed periods $\leq$2 ms. The solid line indicates a single exponential with time constant of 2.3 ms.

Fig. 25 Characteristics of the less prominent small events observed in 50 μM cGMP. a, A 625 ms record showing a number of small amplitude events.[3] The bar to the right of the trace represents $\pm$2 pA. b, Amplitude plot of the record shown in a (squares) compared with a control plot (circles). The non-zero peak has an estimated mean of 1.0 pA. c, Open time distribution of events from the record in a, selected by a window of 0.5-1.4 pA. The solid line is an exponential fit to the data with time constant of 1 ms.

Fig. 24

A.

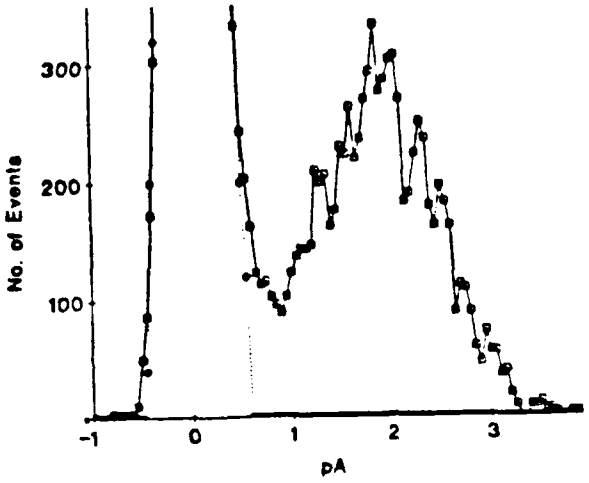
300
200
100
No. of Events
-1
0
1
2
3
pA

B.

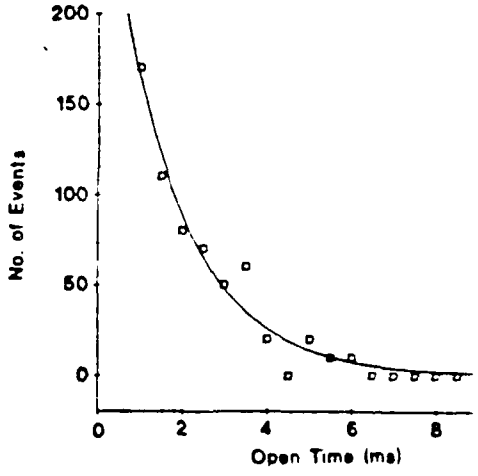
200
150
100
50
0
No. of Events
0
2
4
6
8
Open Time (ms)

C.

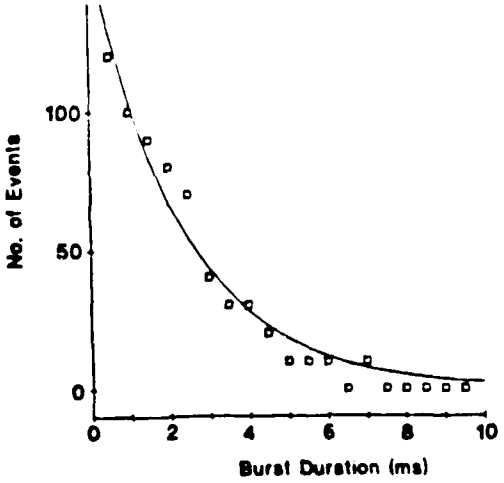
100
50
0
No. of Events
0
2
4
6
8
10
Burst Duration (ms)

Figure 25

A.

B.

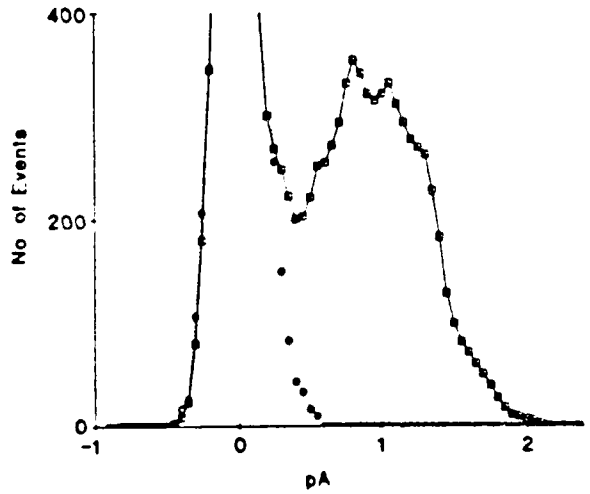

C.

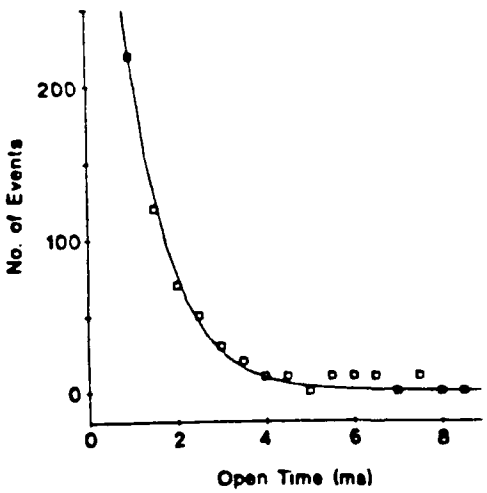

deviation of 0.27 pA. The open time distribution is shown in Figure 25c. The distribution could be fit with an exponential with time course of 1 ms (uncorrected for 2 kHz filtering). It is not clear, at this point, why we do not observe a contribution by this small event to the (2 pA) apparent unit conductance. It is possible that further experimentation and analysis at low cGMP concentrations may reveal a contribution of small events in these areas.

Our results demonstrate that opsin, when reconstituted into phospholipid vesicles, exhibits cGMP-activated single channel activity. In these experiments opsin exhibits cGMP sensitivity and specificity similar to that reported for the cGMP-gated channel studied in patches excised from rod outer segment plasma membrane (Fesenko et al., 1985). The single channel amplitude and kinetic characteristics observed for purified, reconstituted opsin are almost identical to those of the plasma membrane conductance (Haynes et al., 1986; Zimmerman and Baylor, 1986; Matthews, 1987). The only characteristic of the plasma membrane conductance which we have failed to observe in opsin-phospholipid vesicles is a Ca^{2+} blockade (Haynes et al., 1986; Bodoia and Detwiler, 1984). Possible explanations for this discrepancy include species difference (bovine versus amphibian), difference in lipid environment, or an effect of DTT on the protein.

The opsin used in these patch experiments does not appear to have been contaminated with the protein(s) purified by Cook et al. (cf. Figure 22). While contamination with the "39 kdalton" protein of Matesic and Liebman cannot be ruled out, the fact that this "39 kdalton" protein can only be resolved from opsin monomer in SDS gels containing sufficient KCl to precipitate a significant amount of the SDS contained in the gel coupled with the finding that two different anti- rhodopsin polyclonal and two different anti- rhodopsin monoclonal antibodies specifically bind to the "39 kdalton" protein (D. Matesic, personal communication) strongly support the hypothesis that opsin or an opsin multimer can function as a cGMP-activated conductance.

References

Cook, N.J., Hanke, W. and Kaupp, U.B. **Proc. Natl. Acad. Sci. U.S.A.** **84**:585-589 (1987).

Fesenko, E.E., Kolesnikov, S.S. and Lyubarsky, A.L. **Nature** **313**:310-313 (1985).

Harary, H.H., Brown, J.E. and Pinto, L.H. **Science** **202**:1083-1085 (1978).

Haynes, L.W., Kay, A.R., and Yau, K.-W. **Nature** **321**:66-70 (1986).

Kamps, K.M.P., Reichert, J. and Hofmann, K.P. **FEBS Lettres** **188**:15-20 (1985).

Kuhn, H., Bennet, N., Michel-Villaz, M. and Chabre, M. **Proc. Natl. Acad. Sci. U.S.A.** **78**:6873-6877 (1981).

Laemmli, U.K. **Nature** :**227**:680-685 (1970).

Matesic, D. and Liebman, P.A. **Nature** **326**:600-602 (1987).

Matthews, G. **Proc. Natl. Acad. Sci. U.S.A. 84**:299-302 (1987).

Zimmerman, A.L. and Baylor, D.A. **Nature 321**:70-72 (1986).

4. Publications:

Stein, P.J., Halliday, K.R. Chernoff,N., and Rasenick, M.M. (1985) Photoreceptor GTP binding protein mediates fluoride activation of phosphodiesterase. J. Biol. Chem. 260:9081-9084.

Caretta, A. and Stein, P.J. (1985) cGMP- and phosphodiesterase-dependent light scattering changes in rod disk membrane vesicles: Relationship to disk vesicle-disk vesicle aggregation. Biochemistry 24:5685-5692.

Caretta, A. and Stein, P.J. (1986) Light- and nucleotide-dependent binding of phosphodiesterase to rod disk membranes:Correlation with light scattering changes and vesicle aggregation. Biochemistry 25:2335-2341.

Caretta, A. and Stein, P.J. Light- and nucleotide-dependent increase in apparent viscosity in a suspension of retinal disks. FEBS Lettres 219:97-102.

Stein, P.J. and Caretta, A. Light-induced infrared light scattering signal in the retina: Effect of phosphodiesterase inhibitors. (submitted to Journal of Cell Science).

Clack, J.W. and Stein, P.J. Opsin exhibits cGMP-activated single channel activity. (submitted to Nature)

Clack, J.W., Pincus, D.W., and Stein, P.J. Rod GTP-binding protein without bound nucleotide is tightly bound to rhodopsin. (submitted to Biochim. biophys. Acta)

Caretta, A., Kolstad, K., and Stein, P.J. ATP releases 205 Kd neurofilament subunit from brain and retinal neuronal preparations. (manuscript in preparation).

5. Professional Personnel:

Peter J. Stein, Ph.D., Research Scientist
James W. Clack, Ph.D., Associate Research Scientist
Antonio Caretta, M.D., Post Doctoral Associate
Edward W. Karbon. Ph.D., Postdoctoral Fellow

6. Interactions:

ARVO Meeting, May 5-10, 1985, Sarasota, FL.

University of Illinois at Chicago, Department of Physiology and Biophysics, Invited Lecture: Light Scattering Changes in Rod Disk Membranes and Retina. November 13, 1985.

Purdue University, Department of Biological Sciences, Invited Lecture: Light Scattering Changes in Rod Disk Membranes and Retina. October 17, 1985.

ARVO Meeting, April 28 - May 2, 1986, Sarasota FL.

FASEB Meeting, August 11 - 16, 1986, Saxon's River, VT.

Society for Cell Biology, December 7-11, 1986, Washington, D.C.

ARVO Meeting, May 4-8, 1987, Sarasota, FL.

FASEB Meeting, July 26-31, 1987, Copper Mountain, CO.

END

DATE

FILMED

6-88

DTIC